FERMILAB PROPOSAL No. 307

Correspondent: L. T. Kerth

FTS/Com 415 843-2740, Ext 5501

# MUON-NUCLEON SCATTERING WITH EXTRAORDINARY MOMENTUM TRANSFER

A. R. Clark, L. T. Kerth, M. Strovink, W. A. Wenzel

Department of Physics and Lawrence Berkeley Laboratory,
University of California, Berkeley, CA. 94720

Rolland P. Johnson

Fermi National Accelerator Laboratory, Batavia, Ill. 60510

F. C. Shoemaker

Joseph Henry Laboratories, Princeton University,
Princeton, N. J. 08540

May 30, 1974

# I. SUMMARY

The amazing success of parton models which explain SLAC electroproduction results with very few conceptual complexities stimulates us to believe we are on the verge of discovering another level of the basic structure of matter. Indeed, recent results from neutrino scattering experiments at FNAL have confirmed the idea that nucleons are made of smaller constituents. On the other hand, the cross-sections for $e^+e^- \rightarrow$ hadrons measured at CEA and SLAC indicate that the most simple constituent models are almost certainly wrong. At this point, the most straightforward method to see directly the substructure of the nucleon is to bombard it with the simplest probe at the highest possible momentum transfer.

This is a proposal to build a magnetic spectrometer with advanced features, to study the character of μN deep inelastic scattering in kinematic regions which fully exploit FNAL capabilities and yet are not covered by existing experiments. The device consists of slabs of iron sandwiched between scintillation and wire proportional counters. The iron is magnetized and serves both as the momentum analyzer and the target material for the incident muons. The acceptance of the spectrometer is quite uniform and the muon-nucleus cross-sections for 200 GeV incident energy will be measured for momentum transfers to beyond 175 $(GeV/c)^2$.

The spectrometer can quickly be rearranged (or scaled) to give equivalent acceptance and momentum resolution for different beam energies, thus minimizing systematic errors and permitting precise comparisons of data taken at different muon energies. The scintillators between the iron slabs of the spectrometer, used to determine the μN interaction vertex, will be pulse-height-analyzed to measure the total energy of the final state hadrons. This improves the spectrometer resolution and allows a better determination of the nuclear structure function. The apparatus will be modular and versatile and can be used for other experiments such as those described in FNAL proposal 203A.

The experiment has been designed to be used in the present FNAL muon beam and requires $10^{11}$ muons at 200 GeV and $10^{11}$ at 89 GeV. Because fast detectors are used, it can take full advantage of the higher flux available after fall 1974. We propose to start to install the apparatus in March 1975. This allows E-26 to complete its program without disruption. Much of the tune-up can be done parasitically and we hope to take data shortly thereafter.

Table of Contents

## II. PHYSICS JUSTIFICATION

### Introduction

The use of virtual photons to probe the electromagnetic structure of matter is a broad and traditionally fruitful experimental pursuit. At FNAL, muons are a source of photons which can carry uniquely large momentum transfer, probing the nucleon charge structure at shorter distance than heretofore possible. These are the key to exploring the SLAC discovery[1] that, in a limited kinematic range, nucleon inelastic form factors ($\nu W_2$) depend on the photon four-momentum in a manner invariant to energy scale. This observation has led to the invention of relatively structureless nucleon constituents, whose average charge-squared and energy distribution are determined by the structure functions. Recently, an LBL-SLAC experiment at SPEAR[2] has decisively confirmed the earlier trend observed at Frascati and CEA that the cross-section for $e^+e^- \rightarrow$ hadrons has an energy-dependence which is incompatible with the simple versions of these constituent models. By itself, this fact guarantees central interest in the question of scale-invariance in muon scattering at highest $Q^2$; an observed deviation from scaling would help to define the constituent structure, while continuation of the SLAC behavior would create a fascinating anomaly. More generally, carefully executed measurements of nucleon inelastic form factors will answer a host of basic questions. For example, these data will be used to test the specific behavior of $\nu W_2$ predicted by asymptotically free gauge theories[3], and, using CVC, to untangle those features of neutrino-nucleon scattering having mainly to do with structure of constituents from those aspects most related to the (unknown) high-energy behavior of the weak interaction itself.

## Current Status of Muon-Nucleon Scattering

The existing FNAL muon experiments (26 and 98) have accumulated data during the past year, including sizeable periods of running with the muon beam operating at design intensity. At the Winter 1974 APS meeting, K. W. Chen of Experiment 26 presented data showing a spectacular (~40%) deficiency of muon scattering events at $Q^2 \approx 40$ $(GeV/c)^2$, as compared to the scaling prediction. However, this information was based on a highly preliminary analysis[4]. Recently, E-26 has collected data ranging up to $Q^2 \approx 80$. At this point, Experiment 98 has received a comparable integrated muon flux; however, low luminosity associated with the use of a hydrogen target has yielded an insignificant number of events above the SLAC $Q^2$ range. These data do contain valuable information on the hadronic final state. In the future, Experiment 98 plans to use both hydrogen and deuterium targets at a variety of beam energies; members of Experiment 26 are proposing another run at higher energy.

It is appropriate to mention the status of two related experiments. At SLAC, electron scattering data at small $\omega$ have been collected[5] up to $Q^2 \approx 30$; at FNAL, first results on the energy-dependence of the neutrino-nucleon total cross-section have been reported.[6] In neither case has a significant deficiency of events at high $Q^2$ been observed; on the contrary, the neutrino cross-section appears to be rising with energy more rapidly than expected.

## Experimental Philosophy

In designing a second-generation muon scattering experiment at FNAL, one is impressed by the kinematic range intrinsically available. At SLAC, electron scattering data extending to 75% of the maximum $Q^2 = 37\ (GeV/c)^2$ have been obtained. Naively, one could hope to collect data up to $Q^2 = 300$, using 200 GeV muons at FNAL. However, the single factor limiting existing FNAL muon scattering data to 10-20% of the available range is luminosity. Viewed from this perspective, the two-decade improvement in luminosity resulting from use of a nuclear (e.g. iron) target, rather than a hydrogen target, is crucial. Typically, two orders of magnitude in event rate extend the range of $Q^2$ by a factor of almost 3. In the present beam, it is obvious that the information most sensitive to short-distance nucleon charge structure must be obtained using a nuclear target.

For the iron target thickness (18 ft) and $10^{11}$ - 200 GeV muon exposure envisioned in this proposal, Fig. 1 shows the number of events expected above a given $Q^2$, vs. $Q^2$, assuming scaling and unit detection efficiency. It is concluded that the existing muon beam can provide useful data out to $Q^2 \approx 200$, or half the allowable range.

A decision to use a nuclear target is a decision to study a particular mixture of protons and neutrons, in Fermi motion. Fortunately, this same mixture is needed for comparison to FNAL neutrino Experiment 21, and is close to the proton-neutron average used in many sum rules. Fermi motion causes an intrinsic 12% uncertainty in $\nu$. This is not a gross uncertainty compared, for example, to radiative corrections, which, crudely, introduce

a flat 5% low-energy tail on the effective beam energy distribution. Nuclear matter is very transparent to high-$Q^2$ photons, making screening unimportant. In any case, the concept of scale-invariance is as valid for the large collection of possibly pointlike constituents in an iron nucleus, as it is for the small collection in a nucleon.

In addition to Fermi motion, use of an iron target normally introduces some multiple Coulomb scattering, broadening the $Q^2$ resolution. This results in a good match to the resolution (9%-13% in E' and $Q^2$) obtainable in a spectrometer of the magnetized-iron variety long used in cosmic ray experiments. Such spectrometers provide large, flexibly-configured magnetic field volumes at low power consumption and very attractive cost. The resolution functions which must be unfolded in order to extract $\nu W_2(\omega,Q^2)$ do not introduce gross uncertainties compared to the usual radiative corrections. An important exception is the coarse determination of $\nu = E_0-E'$ when E' is more than about half of $E_0$. To analyze this situation an independent calorimetric determination of $\nu$ should be used, making possible a one-constraint fit to all events.

To summarize, we expect that an iron-target iron-magnet muon spectrometer, if carefully designed and systematically understood, can provide the most sensitive information on short-distance nucleon charge structure obtainable in the existing muon beam at FNAL.

## Experimental Design

Design of the proposed muon spectrometer has been defined by four primary objectives. First and most important, we have sought to anticipate sources of systematic error and to make them as small and as understandable as possible. This is especially important for tests of scale-invariance. A second objective has been to provide for an appreciable, slowly varying geometrical acceptance extending over nearly the full range of $Q^2$ and $\nu$ measurable in the existing beam. Third, a second-generation spectrometer must be capable of operation under conditions of highest foreseeable muon beam and halo intensity. This dictates exclusive use of fast proportional-chamber detection planes. Finally, to permit redundancy and uniform measuring error in the determination of $\nu$, a hadron calorimeter has been included as an integral part of the apparatus.

We continue with an elaboration of these points.

Systematic Error. For minimizing systematic errors in a test of scale-invariance, the most important concept is that of a "scale-invariant apparatus." This simple but elegant idea was originated by L. N. Hand and first implemented in FNAL Experiment 26. It consists of varying the apparatus with the muon beam energy so that acceptance and resolution in the scale-invariant variables are constant. This can be achieved, to remarkably high degree, by fixing transverse apertures and average magnetic fields, while varying apparatus length and mass density as $E_0^{1/2}$. Details of the concept appear in Appendix A. Our contribution to the state of this art has been to design a spectrometer for which the transformation between scaled configurations corresponding to two muon beam energies can be accomplished in minutes, without moving detectors. Alternation every few hours between beam energies

can be expected to produce more complete cancellation of systematic bias than is possible without this new feature.

In addition to testing scale-invariance, we wish to extract $\nu W_2(\omega,Q^2)$ by direct comparisons of real and simulated data. Reliability of these comparisons can be enhanced by a variety of monitors and calibrations of the experimental hardware. To this end, it is particularly advantageous to have the beam muons, with their known energy, continuously passing through the magnetized aperture of the spectrometer.

Acceptance. As mentioned above, and indicated in Fig. 1, it is desirable to maintain geometrical acceptance at least out to $Q^2 = 200$, at $E_0 = 200$ GeV. Obviously, angular acceptance of the spectrometer is optimized by maximizing transverse aperture and minimizing length. The latter is accomplished by performing magnetic analysis of the scattered muon in a region as close as possible to the interaction point. Nevertheless, in any economically sensible design, 100% detection efficiency over the whole range of $Q^2$ is not achievable. One is faced with the choice of imposing a major restriction upon either azimuthal or polar scattering angle. It is clear that tight restriction of the polar scattering angle, as usually happens for an apparatus with full azimuthal coverage, is an unwise choice. For example, if at a particular $Q^2$, the detection efficiency is 10%, the spectrometer is almost blind to the 90% of events with highest $\omega$. Restricted azimuthal acceptance, on the other hand, produces a completely uniform attenuation over the $Q^2$-$\nu$ plane. For this reason, we have adopted a configuration providing for generous polar angular acceptance over one azimuthal quadrant.

The most important characteristic of an apparatus which can put the first two objectives within experimental reach is use of a distributed target integral with the spectrometer. Except for a fine granularity,

such a spectrometer is uniform throughout its length; the "scaling change" consists mainly of adding or subtracting unmagnetized material and of redefining the useful length. Use of a long target greatly benefits the luminosity. Throughout the target, each interaction is reconstructed with uniformly high acceptance, using only a short portion of the spectrometer lying immediately downstream of the vertex.

Resolving Time. At $E_0$ = 150 GeV, the existing muon beam already has produced instantaneous halo intensities exceeding 3 MHz. Further intensity improvement within the lifetime of a second-generation muon experiment could quintuple this figure, giving $\sim$ 15 background tracks within a 1-μsec spark-chamber time window. There is no practical alternative to the exclusive use of some type of proportional chamber as a position detector. A straightforward and economically viable plan is to use approximately $10^4$ single-wire-readout proportional chamber channels of conventional design, able to withstand any foreseeable halo intensity in the Muon Lab.

Calorimetry. The muon energy transferred to hadrons, $\nu$, is valuable information amenable to independent calorimetric measurement, as in the FNAL neutrino experiments. This information provides a constrained fit to all events, and supplies the most accurate determination of $\omega$ in the case in which the incident and scattered muon energies differ by less than a factor of two. The design of the calorimeter has benefited from its early inclusion in plans for the proposed spectrometer, and is fully discussed in Appendix C.

## Spectrometer

We have designed the apparatus to be compatible with the FNAL muon beam. It will be located in the downstream half of the Muon Laboratory in the area presently occupied by the equipment of E-26.

The spectrometer has been designed to be scale-invariant for two energies with the ratio $E_1/E_2 = 4/9$. An intense beam of 200 GeV muons will be obtainable in the Muon Laboratory by the fall of 1974; to be conservative, we have used this as the higher energy in design calculations. The lower energy for the test of scale-invariance then would be 89 GeV. However, we are anxious to run at the highest possible energy consistent with adequate flux ($5 \times 10^5$ muons/pulse), with our lower energy scaled accordingly; both the acceptance of the spectrometer and the intrinsic rate at highest $Q^2$ improve as the energy increases. This is discussed in more detail below.

The apparatus we are proposing is a solid-core single-arm spectrometer, with the first part of the spectrometer used as an integral, distributed target. The system is made up of a number of magnetized steel plates, zinc slabs, multiwire proportional chambers and scintillation counters, arranged as shown in Figures 2, 3 and 4.

The magnet structure consists of 72 4-inch thick steel plates, similar in shape to a filament transformer core (see Fig. 4), and magnetized to an internal field of 19 kG by a single coil wound through the entire assembly. The magnet construction is discussed in more detail in Appendix B.

One of the requirements of a scale-invariant apparatus is the ability to change the average density without changing the average magnetic field. This is accomplished by interspersing 36 4-inch zinc slabs through the system, arranged so that a zinc slab follows every second steel plate (see

Fig. 3). In order to scale the apparatus, the zinc slabs are mounted on rollers attached to the steel, such that the zinc can be moved easily in and out of the active area of the spectrometer. Note that the zinc needs to cover only the active area between the coils, and not the return yoke. With the slabs in place, 1/3 of the interactions will occur in zinc; we expect no difference compared to those in iron. If any differences do exist, they can be readily ascertained and the effects studied because the calorimeter counters will localize the interaction to within one plate.

Note that the magnetic field is horizontal, to deflect the muon beam downward. This orientation was chosen to facilitate the support structure for the zinc plates (it is easier to move them horizontally than vertically), and to allow improved access to the counters and chambers.

Multiwire proportional chambers (MWPCs) are placed after every 2 feet of material to provide muon trajectory measurements. Each chamber has an active area of 51 inches wide by 42 inches high, with three sensitive planes (u, v, w). A total of 10,700 channels is required; this number is sufficient to provide a resolution of 0.04 inch in the bending plane and 0.10 inch perpendicular to the bending plane.

The target region contains scintillation counters interspersed every 4 inches with the solid plates to form a hadron calorimeter. The pulse height of each of these counters will be recorded to provide a direct measurement of $\nu$. In addition, the onset of the hadron cascade is used to determine in which plate the interaction occurred. This is necessary because the first two proportional chambers downstream of the interaction may contain many tracks from the cascade which obscure the muon trajectory. If any events should occur without an accompanying hadron cascade, the

nearby chambers will be clean and can be used to find the vertex location. A detailed discussion of the calorimeter can be found in Appendix C.

Four sets of counter hodoscopes ($T_1$-$T_4$) for triggering on scattered muons are located after 15 feet of material, and every 6 feet thereafter. Additional proportional chambers and scintillators will be placed upstream of the spectrometer to define the incident muon trajectory and to provide a veto on the beam halo.

We anticipate the use of a "fast-slow" trigger, the fast trigger consisting of a coincidence between signals indicating the presence of an incident muon, the absence of a muon in the beam halo, and the presence of a scattered muon downstream. Referring to Fig. 4b, the scattered muon signal is defined as at least one count in $T_{ib}$, $T_{ic}$, or $T_{id}$ and no signal from $T_{ia}$. The fast trigger will strobe the detectors into registers; more detailed correlations will then be checked to determine if the event should be recorded.

The configurations of the spectrometer for operation at 200 GeV and 89 GeV are indicated in Fig. 2. At 200 GeV, interactions anywhere in the first 18 feet of material can trigger the system; trigger hodoscopes $T_2$, $T_3$ and $T_4$ are used. The next 18 feet of material after the interaction point will be used to momentum-analyze the scattered muon for the test of scale-invariance. Reconstruction will employ five of the available chambers in this region in order to correspond to the configuration used at the lower energy.

To scale the apparatus to a different incident energy, it is necessary to change both the length of the apparatus and its average mass density. For the lower energy, the length of the spectrometer is shortened merely by ignoring the downstream end. The average density is reduced by re-

moving the zinc slabs, which can be rolled out of the spectrometer in a few minutes. It is not necessary to reposition any of the detectors. The target region is defined as the first 8 feet of steel, and only the upstream trigger hodoscopes $T_1$ and $T_2$ are used. The scaled length for muon analysis is 12 feet starting at the interaction point, and contains 8 feet of steel and 5 usable chambers.

The analysis for determination of the structure function will of course utilize all available information for each event. For many events an improved resolution is attainable because more proportional chamber information is present than can be used in a scale-invariant manner. Additional data for this analysis will be collected concurrently at 89 GeV from the 6-foot long target region between $P_6$ and $P_9$ (see Fig. 2).

For each event at each energy, all counter and proportional chamber information will be recorded. The determination of the interaction vertex location and the decision regarding which chambers should be used for the analysis of the event will be made off-line. This scheme provides a continuous monitor of the performance of each counter and chamber; this is necessary to avoid systematic effects due to inefficiencies, since different elements are used for the triggering and analysis in the two scaled configurations. Also, the maximum information is preserved from each trigger for the measurement of the structure function.

## Simulated Performance of the Spectrometer

Extensive simulation of the performance of the proposed spectrometer was carried out in order to study and optimize its acceptance, resolution, and scale-invariance. The Monte Carlo program included the usual physics (Coulomb and μ-e scattering, muon bremsstrahlung, etc.) of muons passing through iron, and made use of a general algorithm for reconstructing the scattered muon momentum. The program used proportional chamber resolutions of $\sigma = 0.04$ inches within and $\sigma = 0.10$ inches orthogonal to the bending plane. It was assumed that the calorimeter counters could localize the longitudinal vertex coordinate to within one 4-inch plate. The beam muons were assumed to be uniformly distributed over a 50 in $^2$ area, with an energy (for the high-energy configuration) of 200 GeV. As discussed previously, this was intended as a conservative choice; to optimize both intrinsic rate and acceptance at high $Q^2$, the maximum beam energy compatible with reasonable intensity should be exploited.

The result of these studies was that the proposed muon spectrometer satisfies our design objectives. Averaged over the range of $Q^2$ accessible to measurement, the resolution in E' is 13.0% and in $Q^2$, 13.2%. Since $Q^2 \approx E_0 E' \theta^2$, one might have expected multiple Coulomb scattering to significantly worsen the $Q^2$ resolution, relative to that in E'. However, a cancellation occurs when the magnetic field of the spectrometer bends the scattered muon back toward the beam line: overestimation of E' correlates with underestimation of θ, reducing the uncertainty in $Q^2$. This same cancellation makes the resolution in $Q^2$ remarkably independent of longitudinal vertex localization; for $10^3$-event samples, no difference in $Q^2$ resolution between vertex localizations within 2 and within 8 inches

could be discerned. The quoted resolutions in E' and $Q^2$ are only slightly different from the 12% resolution due to Coulomb scattering which would obtain if measuring errors were zero everywhere.

Calorimeter resolution has been estimated using another set of Monte Carlo calculations, described in Appendix C. At $E_0$ = 200 GeV and using 4-inch plates, the uncertainty in $\nu$ due to the calorimeter will be, approximately,

$$\sigma(\nu)/\nu \cong .065\ (\nu/E_0)^{-\frac{1}{2}}.$$

This resolution is well-matched to the intrinsic 12% uncertainty in $\nu$ due to Fermi motion in a nuclear target, and is sufficient to allow the calorimeter information to provide the major constraint on $\omega$ in the case that $\nu < 0.5\ E_0$.

The acceptance of the proposed spectrometer is shown in Figs. 5(a) and 6(a). Fig. 5(a) presents the acceptance, averaged over the population in $\nu$ predicted by scale-invariance, as a function of $Q^2$. The curve is extremely well-behaved, varying by less than a factor of two over the range from $Q^2$ = 15 to $Q^2$ = 150. The average efficiency over this wide range is 17%; at $Q^2$ = 200, the efficiency is still 5%. Since 25% is the maximum efficiency obtainable in one quadrant, it is clear that a large fraction of the $Q^2$ - $\nu$ plane is detected almost without efficiency bias. This point is emphasized in Fig. 6(a), which shows 20%, 10%, and 5% acceptance contours in the $Q^2$ - $\nu$ plane. The grid of numbers, representing accepted events after uniform generation on the plane, further illustrates the slow variation in detection efficiency.

Scale-invariance of the spectrometer implies that the acceptance, expressed as a function of $Q^2/s$ and $\nu/E_0$, is the same at $E_0$ = 89 GeV as at

$E_0$ = 200 GeV. The principal known sources of non-scale-invariant behavior are: calorimetry, radiative corrections, energy-dependent dE/dx, unscaled longitudinal vertex localization, and granularity of the scaling transformation. For direct comparison of data obtained at the two-beam energies, we do not now envision using the calorimeter information, although we are continuing to study possible methods of making that information "scale." The last four enumerated sources of non-scaling are small and calculable. In particular, we re-emphasize the insensitivity of the $Q^2$ resolution to precision of longitudinal vertex localization. A preliminary Monte Carlo simulation without radiative corrections, appropriate to an earlier and much more granular version of the proposed apparatus, verified its scale-invariance to within approximately 5% over the range of $Q^2/s$. In view of the improvements which have been possible, this level of scale-noninvariance should be regarded as a conservative upper limit.

## Rates and Sensitivity of the Experiment

The table below shows the number of events expected for a $10^{11}$-muon illumination of the spectrometer, assuming scale-invariance and (a) $E_o$ = 200 GeV, or (b) $E_o$ = 250 GeV. At $E_o$ = 200 GeV, 100 events are obtained above $Q^2$ = 160; at 250, 100 events are above $Q^2$ = 200. Obviously the 25% increase in beam energy is worthwhile.

| (a) $E_o$ = 200 GeV | | (b) $E_o$ = 250 GeV | |
|---|---|---|---|
| $Q^2$ $(GeV/c)^2$ | Events above this $Q^2$ | $Q^2$ $(GeV/c)^2$ | Events above this $Q^2$ |
| 40 | 25,000 | | |
| 60 | 14,800 | 60 | 22,700 |
| 80 | 8,950 | 80 | 10,200 |
| 100 | 2,340 | 100 | 4,980 |
| 120 | 905 | 120 | 2,480 |
| 140 | 310 | 140 | 1,200 |
| 160 | 115 | 160 | 605 |
| 180 | 33 | 180 | 270 |
| | | 200 | 110 |
| | | 220 | 43 |

The sensitivity of this experiment to physical effects can be explained for two kinds of scenario. In the first, $\nu W_2$ could have a high-$Q^2$ dependence at fixed $\omega$ which does not vary strongly with $\omega$. This sort of scaling violation would show up in the "natural" integral over $\omega$ (approximately $\int \omega^{-1} \nu W_2(\omega, Q^2)\, d\omega$ ) obtained by summing up all events obtained in a particular $Q^2$ band. When the data above a particular $Q^2$ are compared to Monte Carlo, the fractional statistical error is just $N^{-\frac{1}{2}}$, where $N$ is the number of events above that $Q^2$, as found in the above table. On the other hand, we also will compare data taken at $E_o$ with data collected using a scaled apparatus at $4E_o/9$. In that case, the fractional statistical error

on the ratio will be $(N/2)^{-\frac{1}{2}}$. Moreover, a slowly varying scaling violation would not produce as large a deviation in the ratio of data taken at different beam energies, as it would in the ratio of data to Monte Carlo. The difference in the deviations would depend on the type of scaling violation. An example would be a scaling violation of the form $(1 + Q^2/\Lambda^2)^{-2}$ in $\nu W_2$, with $\Lambda$ = 37 GeV. Assuming $E_0$ = 200 GeV, and considering all $Q^2$ greater than 120 $(GeV/c)^2$, one would have a ratio of $E_0$ = 200 GeV data to Monte Carlo of $0.83 \pm 0.028$, and a ratio of $E_0$ = 200 GeV data to "scaled" $E_0$ = 89 GeV data of $0.90 \pm 0.042$.

In this first scenario, systematic errors would be of two main types. First, there would be uncertainty in the overall detection efficiency. By taking care with the hardware and reconstruction algorithms, we expect to limit our uncertainty to $\pm$ 4% in absolute detection efficiency and $\pm$ 2% in relative efficiency for different beam energies. Second, finite resolution in $Q^2$ could mask spikes, steps, etc. in the $Q^2$-dependence of $\nu W_2$, if these pathologies were characterized by $\Delta Q^2/Q^2 \ll 13\%$. But for gentle scaling violations of the kind parameterized above, the $Q^2$ resolution produces only a small dilution of the effect.

In the second kind of scenario, the $Q^2$-dependence of $\nu W_2$ at fixed $\omega$ could vary strongly with $\omega$. Here one is faced with the general problem of unfolding the resolution functions and radiative corrections to obtain $\nu W_2(\omega, Q^2)$. Without a particular scaling violation and unfolding algorithm in mind, we can make only general observations: (1) This sort of procedure would be attempted first for comparisons of data to Monte Carlo, since the calorimeter information, used heavily to determine $\omega$, does not scale. (2) Avoiding excessive systematic error in the unfolding process requires excellent knowledge of the resolution functions, which should be measured

independently wherever possible. (3) Unless $\nu/E_0 \lesssim 0.15$, these resolutions are not gross compared to the smearing associated with radiative corrections unfolded for e-p scattering at SLAC, making the procedure appear quite manageable. (4) A particularly attractive strategy would be to construct a polynomial parameterization in $\omega$ of $\nu W_2(\omega,Q^2)$ for a number of $Q^2$ bands. Then the polynomial coefficients and their error matrix would immediately determine the oft-mentioned structure function moments

$$B_n(Q^2) = \int \omega^{-2n-2} \nu W_2(\omega,Q^2)\, d\omega.$$

The fractional statistical error in $B_{-\frac{1}{2}}$ would be approximately $N^{-\frac{1}{2}}$, where $N$ is the number of events in the $Q^2$ band (see the table above). Higher moments would have larger errors.

## Comparison with Other Experiments

We have considered modifications to the existing apparatus of Experiments 26 and 98 which might accomplish the experimental objectives of this proposal. Briefly restated, these objectives are: good control over systematic errors; geometrical efficiency extending to $Q^2 = 200$; ability to use the highest muon flux; and redundant calorimetric measurement of $\nu$. These are accomplished in the proposed apparatus by using a long target integral with the spectrometer. This longitudinal uniformity makes it possible to "scale" the apparatus quickly without moving detectors, and to obtain an acceptance which is constant as a function of vertex position along the target. In addition, the proposed experiment has gained acceptance in scattering angle by restricting the azimuth to one quadrant. Fig. 5a shows the acceptance, which averages 17% and varies by less than a factor of two over the range of $Q^2$ from 15 to 150 and is 5% at $Q^2 = 200$. Multiwire proportional chambers are used throughout to allow good time resolution, and calorimeter counters are distributed uniformly through the spectrometer.

Below, we discuss each of the E-26 and E-98 spectrometers in turn: first in their present configuration; second, with possible modifications which would attempt to satisfy the above criteria. The detailed assumptions that we have made about these spectrometers are given in Appendix D. For the comparisons we have assumed a muon beam energy of 200 GeV. However, we emphasize that the highest possible energy compatible with reasonable fluxes ($\sim 5 \times 10^5$/pulse) increases the kinematic range available for all apparatus.

Experiment 26. The geometrical efficiency of E-26 in its normal configuration (8 magnets and the ability to scale) is shown in Fig. 5b for both a 3-ft and an 18-ft target. It is seen that this apparatus does not have the capability of detecting events much above $Q^2 = 120$.

This apparatus could be used in a non-scaling mode in which only the first 3 magnets are employed. An 18-ft target could replace the usual 3-ft. target to obtain luminosity equal to that of the proposed new spectrometer. The spark chambers could be replaced with proportional chambers ($\sim$ 20,000 wires). Using this shorter configuration would increase the angular acceptance and thus the $Q^2$ range; our calculation of the acceptance over the $Q^2$-$\nu$ plane is shown in Fig. 6c. It is seen that this configuration would achieve a cutoff at large $\nu$ for a given high $Q^2$ which is essentially the same as that of our proposal (Fig. 6a). However, what must be paid for this achievement is an experiment which is very sensitive to systematic errors. Use of the long target (18') which is not integral with the detector (as it is in the proposed spectrometer) would give an angular acceptance which varies by a large amount with the position of the interaction along the target. This would result in an acceptance that is a strong function of $\nu$ and $Q^2$. This nonuniform acceptance would make the loss of the "scale invariant" feature even more serious. Comparison of the cross-sections at different beam energies would be critically dependent on Monte Carlo simulation of the apparatus. For these reasons, we have rejected this use of the Experiment 26 apparatus.

Muon Scattering Facility (E-98). In its present configuration, the apparatus of E-98 has neither the luminosity nor the kinematic range to achieve our experimental goal. As can be calculated from Fig. 1, an exposure of $10^{11}$ muons with unit acceptance and a 1-meter liquid hydrogen

target would produce 2000 events above $Q^2$ = 15 $(GeV/c)^2$ rather than the same number above $Q^2$ = 150 $(GeV/c)^2$, as would be possible for an 18-ft iron target. In addition, the acceptance (Fig. 5d) falls to 5% at $Q^2$ = 120 and there is no appreciable acceptance above $Q^2$ = 150.

The modifications that would be required are extensive. First, the hydrogen target would have to be replaced by a heavy target to increase the luminosity. To improve the acceptance, it would be necessary to increase the efficiency for large scattering angles, for example, by making the apparatus more asymmetric in azimuth. This could be done by reversing the Chicago cyclotron magnet. Unfortunately, this deflects the muon beam into Road A, creating a radiation hazard. Alternatively, the downstream spark chambers could be moved east. This would require major displacement of the wall and foundation of the muon laboratory. Another possibility that would increase the E-98 angular acceptance would be to shorten the apparatus by moving the rear spark chambers and 1000-ton muon filter upstream.

All of these possibilities have fatal drawbacks. First, they are expensive and would substantially disrupt the very important program of E-98. Also, multiple Coulomb scattering in a heavy target limits the resolution in $Q^2$ such that the high resolution afforded by the cyclotron magnet is not needed. The spark chambers of the facility do not provide sufficient time resolution to operate the proposed experiment for even a modest increase in beam halo flux. To replace these large chambers with proportional chambers is financially infeasible. Finally, the modified apparatus would not have the scale invariant property of the proposed spectrometer.

In summary, we see that neither E-26 nor E-98, even with extensive modifications, can provide the proper combination of rate, geometrical acceptance, and control of systematic error needed to achieve the goal of an optimal test of scaling at highest $Q^2$.

## III. APPARATUS NEEDED

The spectrometer and detectors have been described in detail in the preceding section. Our experimental collaboration will assume responsibility for the design, construction, and funding of the scintillation counters, proportional chambers and specialized electronics. The magnet assembly would be funded by FNAL, with the design and supervision of outside work to be done by us. We will require a PDP-11 computer from FNAL.

Magnet Assembly. The magnet structure (see Figs. 3 and 4 and Appendix B) will require 72 4-inch thick steel plates of outside dimensions 7 feet x 8 feet and total weight of 330 tons before the coil slots are flame-cut. Distressed steel stock is acceptable. While steel prices have been changing rapidly, distressed steel has been selling recently for about $150/ton, giving a cost of $49,500 for the magnet steel. The assembly will require 40 tons of zinc, formed into slabs approximately 42 inches x 51 inches x 4 inches. Zinc was recently purchased by FNAL for the neutrino laboratory for about $0.30/lb., which would result in a cost of $24,000 for the material required here. The coil will require 6300 pounds of hollow aluminum conductor at an estimated cost of $7,600. Final fabrication costs are not included in the above figures.

The design of the magnet assembly will be done by the collaborating groups. Fabrication would probably be done most economically in the Chicago area, with supervision of the outside contractors done by us. Funding for materials and fabrication costs would come from FNAL. We will also need assistance from the FNAL staff for the installation of the magnet assembly. The magnet power supply would be provided by FNAL. The final design parameters of the coil can be adjusted to match available power supplies.

Scintillation Counters. Sufficient supplies of plastic scintillator, photomultiplier tubes and tube bases to meet the needs of this experiment can be obtained from an existing spectrometer at LBL.

Proportional Chambers. The proportional chambers will have to be designed and built; because of the relatively coarse spatial resolution required, we expect these to be relatively inexpensive. The chambers will require 10,700 channels of read-out electronics; 4100 channels have been built at LBL for earlier experiments and will be available for use here. Also available will be an additional 2200 channels of fast delay cable which are owned by Princeton and have been used in E-26. The remaining channels will be newly constructed, using as inexpensive an electronics design as possible.

Logic. Much of the required electronics can be assembled from existing components at LBL and Princeton. We expect to borrow a modest quantity of fast electronics from PREP.

On-line Computer. We will need a PDP-11 computer from the FNAL pool for on-line data acquisition. We do not anticipate any non-standard requirements. Magnetic tapes will be supplied by the experimenters.

We also expect to use the NAL CDC-6600 for fast off-line checks of the data and the performance of the apparatus. The actual data analysis will use our home computers.

## IV. SCOPE

Design and Construction. The design and fabrication schedule is shown in Fig. 7, assuming approval of the experiment is forthcoming in mid-July. The design and construction of the proportional chambers, specialized electronics and counters will be carried out and funded by the experimental groups.

The design and supervision of the construction of the magnet and zinc slab assembly will be the responsibility of the experimental groups. The funding would be from FNAL. We would expect the heavy construction to be done in the Chicago area and plan to have personnel available for adequate supervision and inspection of the work of the vendor. As seen from Fig. 7, installation in the muon lab could start in mid-March, 1975. We would need the assistance of the FNAL staff for the installation of the magnet assembly. Light assembly of the rest of the apparatus will be the responsibility of the experimental groups.

Testing and Debug. For testing and debug of the apparatus we will need about 2 weeks of beam time, of which approximately 90% could be parasitic to Experiment 98.

Running Time. In the data taking mode we require runs of $10^{11}$ muons at each of the two energies 89 GeV and 200 GeV. As stated above we require alternation between the two energies every few hours with the time split approximately equally between $\mu^+$ and $\mu^-$. With the assumptions of $2 \times 10^6$ muons/pulse and 500 pulses/hour, this leads to a beam time of 200 hours.

As stated above, the energies of 89 and 200 GeV are taken as examples for the calculations of this proposal. If operation at significantly higher energy than 200 GeV becomes feasible, a substantial improvement can be achieved in the measurable range of the kinematic variables. We will take data at the highest energy above 200 GeV that is practical. For the

test of scaling, the lower energy to be used is 4/9 of that used for the high-energy point.

Personnel. In addition to the above named physicists, the experimental group involved in this experiment will consist of:

2 additional Ph.D.'s

2 graduate students

5 technicians.

This effort will be our major commitment for the next several years.

## Future Plans

Proposal 203A. The magnets and proportional chambers mentioned above are the same as those proposed to study multiple-muon final states as produced by neutral heavy lepton decays and virtual Compton scattering (FNAL proposal 203A). These experiments naturally are viewed as a straightforward extension of the experiment which has been discussed in this proposal. The changes in the apparatus which will be necessary to do 203A are as follows: the zinc slabs will be removed and the spectrometer correspondingly shortened to increase the acceptance. The trigger will be changed from the requirement that one muon scattered out of the beam to the requirement that more than one muon was produced in an interaction. Finally, the beam will be centered on the active area of the spectrometer and the calorimeter scintillators repositioned.

Although proposal 203A calls for 5 times as many muons as in this present proposal and an apparatus which is twice as long, it is true that the necessary flux could be obtained by running parasitically with E-98. It should also be noted that the muon flux estimates upon which proposal 203A was based are more easily envisioned at present.

Neutral Currents. As a method of seeing weak neutral currents in charged lepton interactions, we have been considering the possibility of searching for parity violating effects in $\mu N$ interactions. To see such effects we believe that one needs to have control over the polarization of the incident muon beam and good sensitivity for events with large $Q^2$. Clearly the $Q^2$ sensitivity is provided by the apparatus which we are proposing to construct, but the questions of muon polarization and the requisite apparatus symmetry are more complex.

Such an experiment would consist of measuring the μN cross-section at high $Q^2$ with two different muon polarizations. Any difference would be a manifestation of weak-electromagnetic interference. The experimental difficulty is to insure that the muon polarization is the only independent variable in the two measured cross-sections.

In practice, there are two feasible methods of obtaining muons of a particular momentum with different polarizations. One method, now being used by Landsberg and collaborators at Serpukhov, involves selecting the momentum and thereby polarization, of muons decaying from a monoenergetic $\pi^+$ beam. By using two different $\pi$ energies, it is possible to get oppositely polarized muons at an energy close to one-half the maximum available energy. This method has the disadvantage that the available $Q^2$ is not the maximum possible for a particular accelerator. The difference in μN cross-sections for different incident muon polarizations has been calculated by Berman and Primack[7] using the Weinberg model. It is found that the asymmetry of the counting rates varies linearly with $Q^2$ and is an extremely sensitive measure of the Weinberg angle, $\theta_W$:

$$\frac{d\sigma(\mu_L^- N) - d\sigma(\mu_R^- N)}{d\sigma(\mu_L^- N) + d\sigma(\mu_R^- N)} = -K\left(\frac{Q^2}{100\ \text{GeV}^2}\right) ,$$

where, for $\sin^2\theta_W = 0.3$, the best value at present, K = 0.2%. For $\sin^2\theta_W = 0.4$, K becomes 3.2%.

The other possible method of obtaining muon beams with different polarizations is to use muons with opposite charges. Given that there is some momentum selection of the muons from $\pi^\pm$ decay, the different helicities of the associated neutrinos insure that the $\mu^+$ will be polarized oppositely to the $\mu^-$. The asymmetry in counting rates due to weak-electromagnetic

interference has also been calculated using the Weinberg model.[7]

$$\frac{d\sigma(\mu_L^- N) - d\sigma(\mu_R^+ N)}{d\sigma(\mu_L^- N) + d\sigma(\mu_R^+ N)} = -(1.4\%)\left(\frac{Q^2}{100\ \text{GeV}^2}\right)$$

In this case, the major difficulty is that the muon polarization is not the only variable. M. Suzuki[8] has estimated the asymmetry expected due to the difference in the muon charges. Although the absolute value of the 2 photon-one photon interference terms are difficult to estimate for inelastic scattering, he has advised us that the $Q^2$ dependence is different than in the weak-one photon case and so the two effects are, in principle, separable. In fact, S. Brodsky[9] has suggested to us that those two photon-one photon interference terms which are difficult to calculate are scale invariant when viewed in a parton model. On the other hand, the weak-one photon interference leads to an asymmetry which is linear in $Q^2$, as noted above. Thus, if the asymmetry measurement were done using a scale invariant apparatus, the contributions due to weak-one photon interference would be directly separable from those due to two photon-one photon interference.

In either of the two cases discussed above, it must be emphasized that the experiment would be a measurement of an asymmetry. And, for such an experiment, all the techniques involving apparatus symmetry which are so well known in high energy physics could be applied. For example, if the incident muon beam were directed down the middle of the apparatus described in the main body of this proposal, the detector would be up-down symmetric, giving the same acceptance for $\mu^+$ and $\mu^-$ without changing $\vec{B}$. Higher order imperfections in the up-down symmetry of the apparatus could be diminished by periodically reversing the magnetic field of the spectrometer.

Using either of the two muon beams with variable polarization mentioned above, we anticipate that an experiment can be designed such that the accuracy of the measurements will be dominated by the statistics. Further, we are sure that such measurements are essential to the understanding of the character of the weak interactions. We expect to pursue the exciting prospect of seeing the weak-neutral-current-induced interactions of charged leptons by submitting a complete proposal in the future.

## REFERENCES


1. E. D. Bloom, D. H. Coward, H. DeStaebler, J. Drees, G. Miller, L. W. Mo, and R. E. Taylor, Phys. Rev. Lett. 23, 930 and 935 ( 1969).

2. A. Litke, G. Hanson, A. Hofmann, J. Koch, L. Law, M. E. Law, J. Leong, R. Little, R. Madaras, H. Newman, J. M. Paterson, R. Pordes, K. Strauch, G. Tarnopolsky, and Richard Wilson, Phys. Rev. Lett. 30, 1189 ( 1973 ).

   SLAC-LBL SPEAR MAGNETIC DETECTOR COLLABORATION, Bull. of Am. Phys. Soc. 19, 542 ( April 1974 ).

3. David J. Gross, Phys. Rev. Lett. 32, 1071 ( 1974 ).

4. See Physics Today, April, 1974, p.17.

5. R. Taylor (private communication).

6. B. Barish, reported at the Fourth International Conference on Neutrino Physics, Philadelphia, Pa. (1974).

7. S. M. Berman and J. R. Primack,"Weak Neutral Currents in Electron and Muon Scattering", SLAC Preprint SLAC-PUB-1360 (T/E) Dec. 1973, (submitted to Phys. Rev. Comments).

8. M. Suzuki, Nuc. Phys. B70, 154 ( 1974 ).

9. S. Brodsky, private communication.

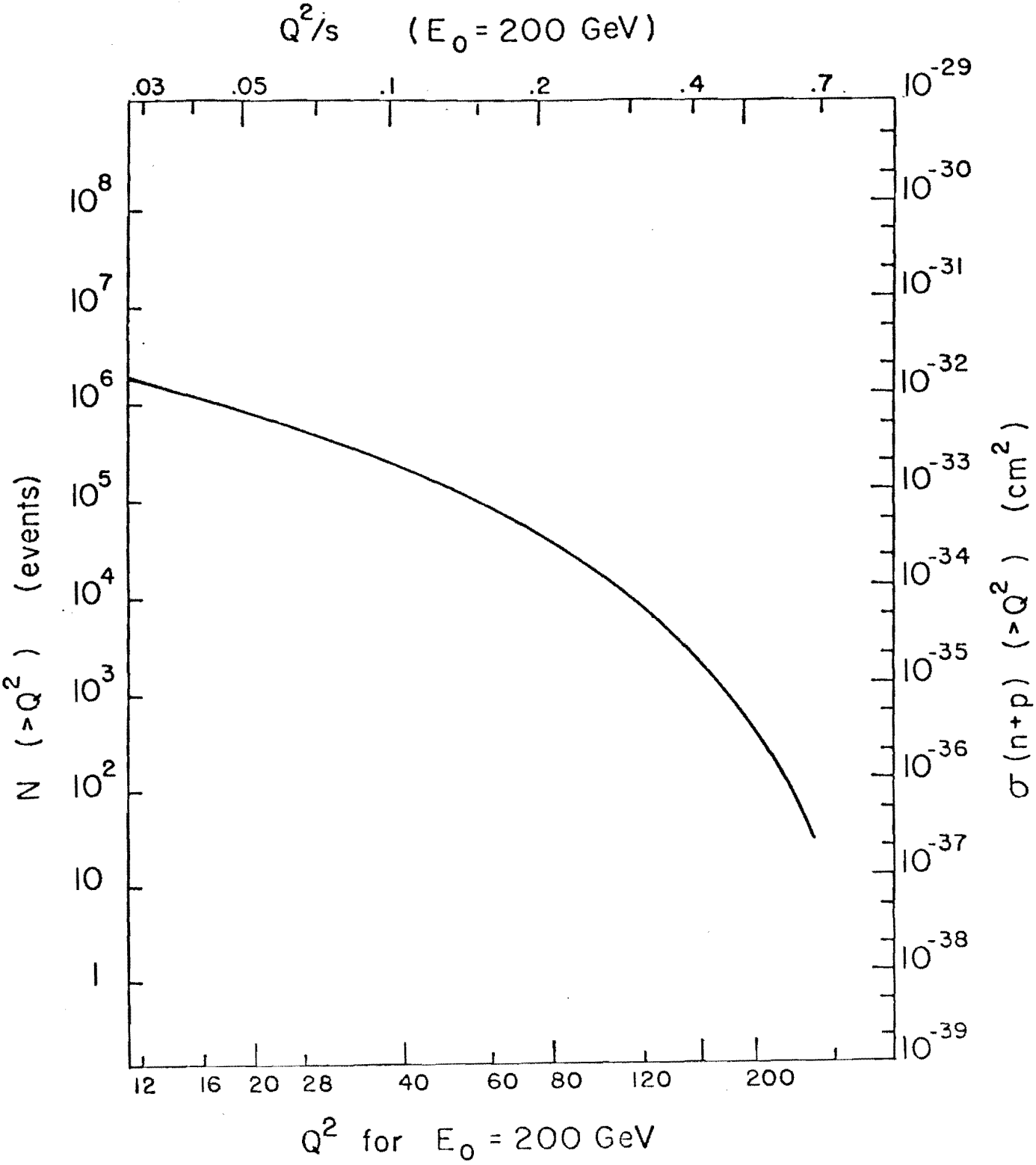


FIGURE 1. The curve shows the number of events expected above a given $Q^2$, as a function of $Q^2$, assuming scale-invariance, an 18-foot iron target, $10^{11}$ incident muons at 200 GeV and unit detection efficiency.

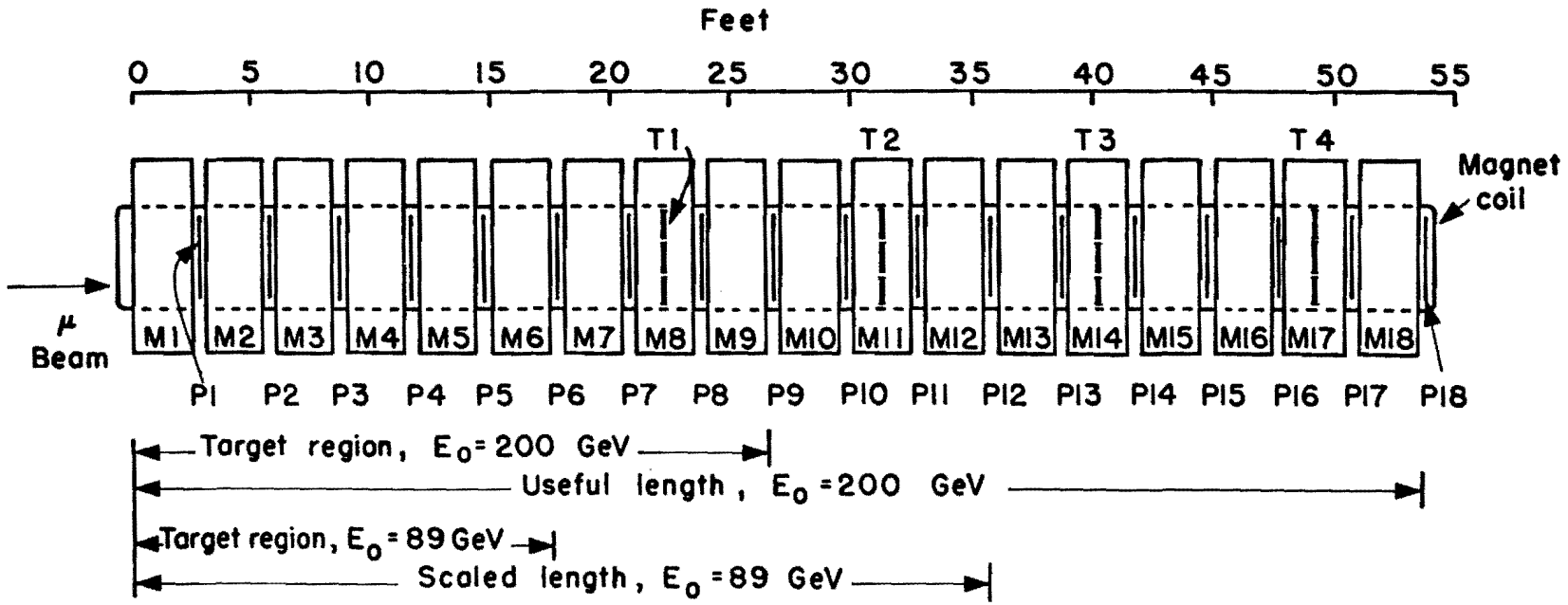


FIGURE 2. Elevation view of spectrometer.

M1 - M18 are assemblies of solid steel "filament transformer" magnet plates, zinc slabs, counters. See the next 2 figures for more detailed drawings. The zinc slabs in M1 through M12 are removable for scaling. The magnets are always saturated.

P1 - P18 are multiwire proportional chambers with 3 sense planes (u,v,w). Total channels - 10,700.

T1 - T4 are trigger hodoscopes.

Calorimeter counters (not shown) are interleaved in the region M1 - M11 (see next figure).

200 GeV configuration:

All zinc slabs in place.
Target region is M1 through M9.
Trigger counters T2, T3 and T4 are used.

89 GeV configuration:

Apparatus downstream of P12 is ignored.
Zinc slabs in M1 - M11 are removed.
Target region is M1 through M6.
Trigger counters T1 and T2 are used.

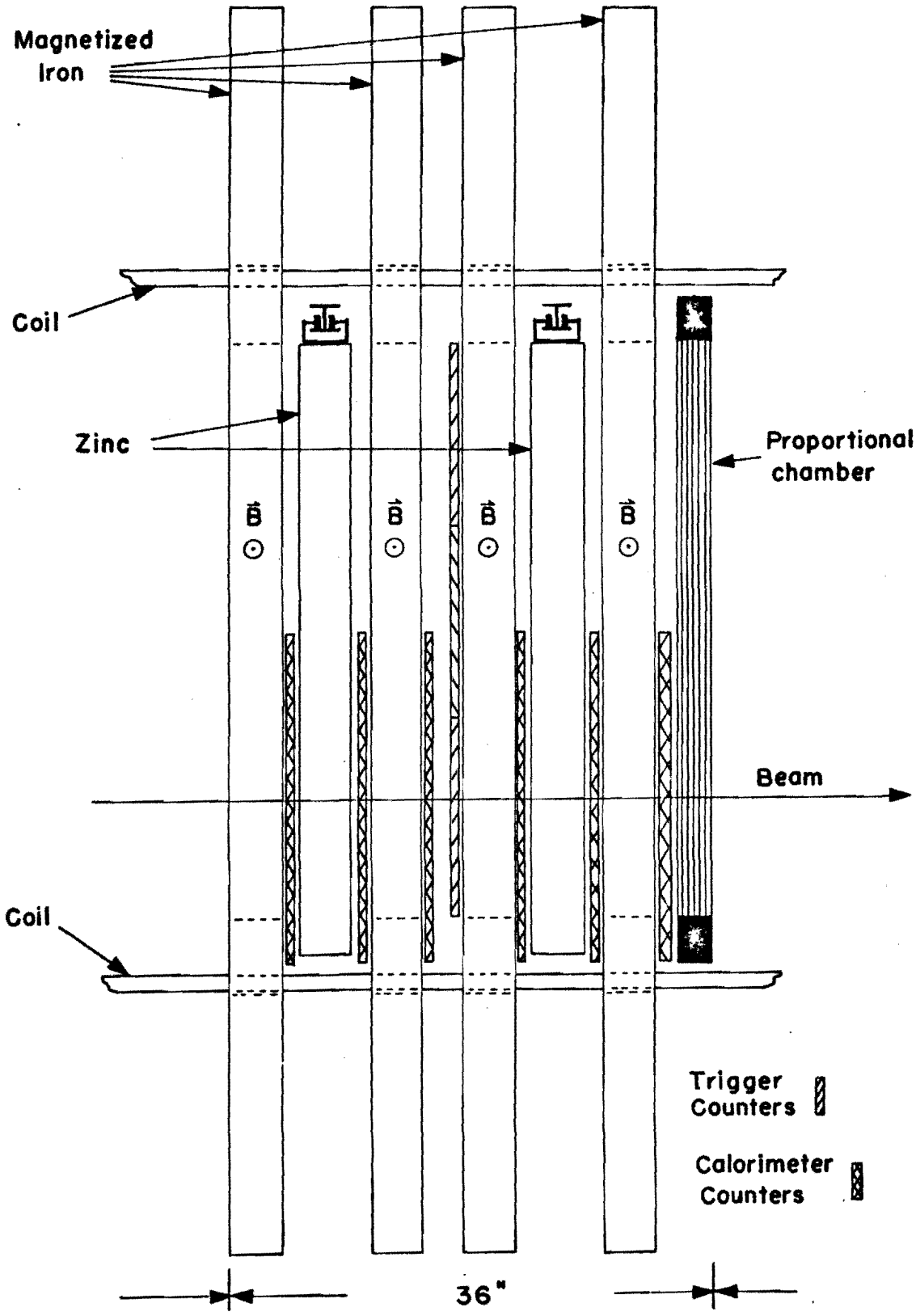


FIGURE 3. Detail of spectrometer construction, elevation view. The spectrometer consists of 18 of these units.

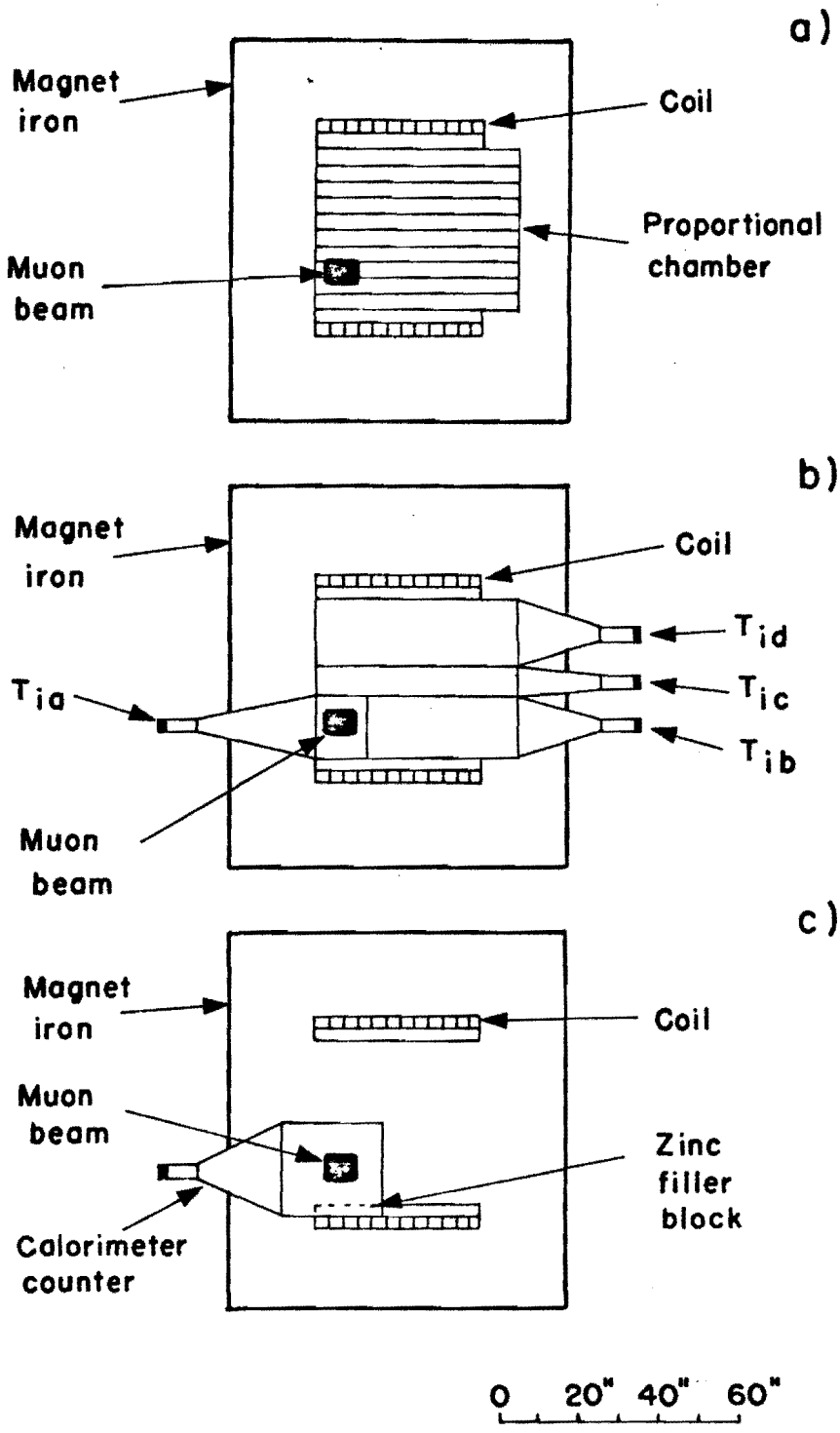


FIGURE 4. Section views of spectrometer, viewed from upstream, showing sizes and transverse locations of a) the proportional chambers, b) the trigger counters, and c) the calorimeter counters.

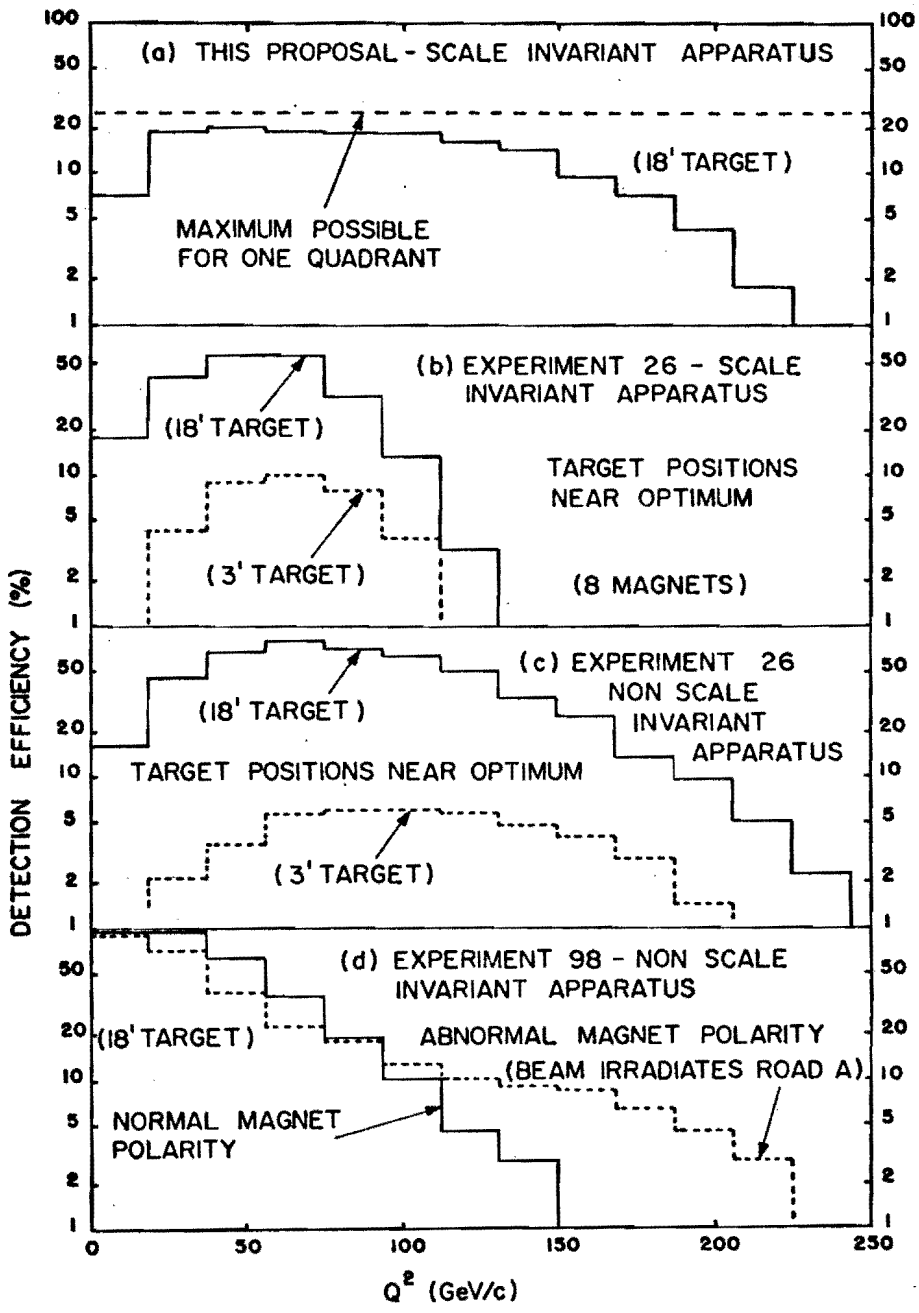


FIGURE 5. Detection efficiencies vs. $Q^2$ at $E_o$ = 200 GeV, for this proposal and variations of other existing equipment (see main text and Appendix D).

a) This proposal - 18-ft iron target, scale-invariant apparatus;

b) Apparatus of E-26, scale-invariant configuration; solid curve - 18-ft target; dashed curve - 3-ft target (this curve has been divided by 6 to reflect the loss in rate of the shorter target);

c) Non-scale-invariant version of E-26 apparatus; solid curve - 18-ft target; dashed curve - 3-ft target (this curve has been renormalized as in b) above);

d) Apparatus of E-98, but with an 18-ft iron target; solid curve - normal magnet polarity; dashed curve - reversed magnet polarity (the muon beam is bent toward Road A).

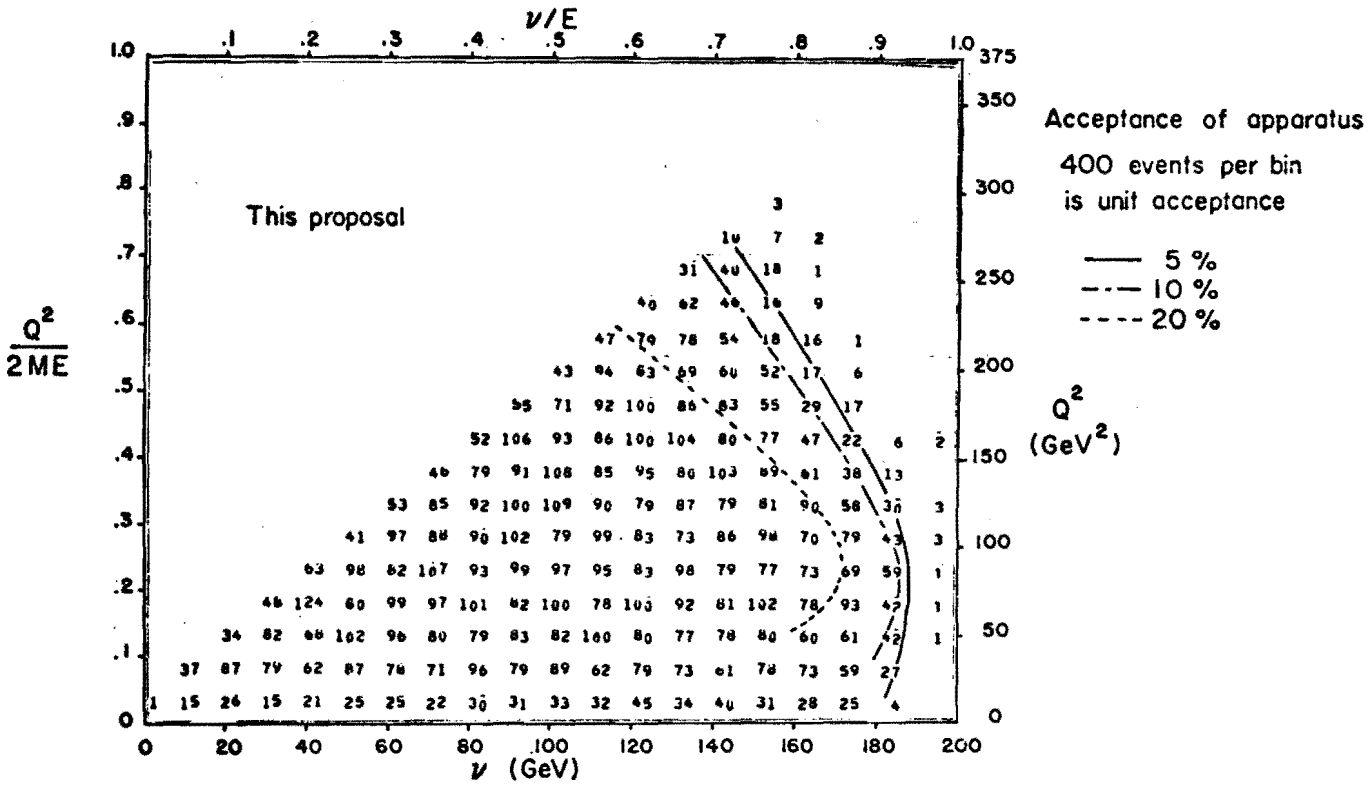


FIGURE 6a. Detection efficiency contours in the $Q^2$ - $\nu$ plane for $E_0$ = 200 GeV using 18 ft target, for this proposal (scale invariant apparatus).

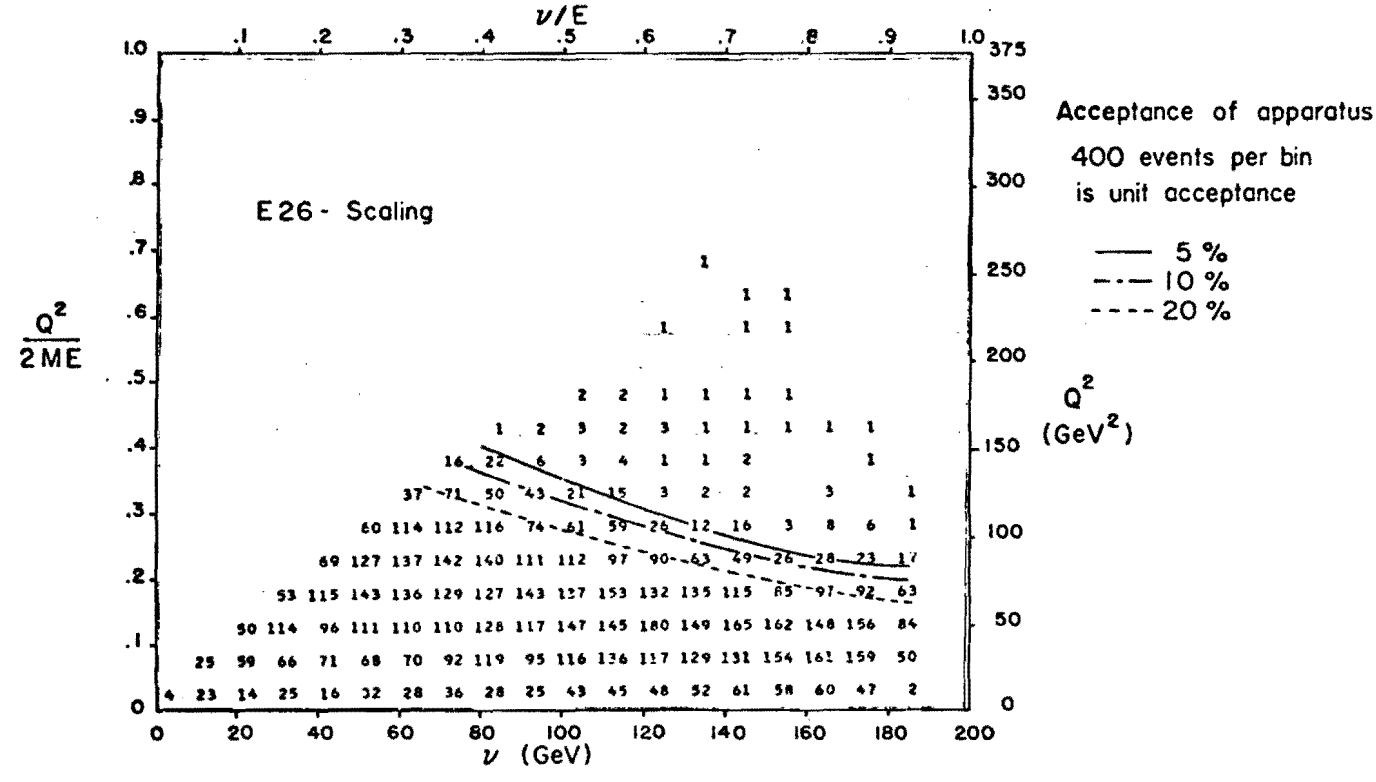


FIGURE 6b. Detection efficiency contours in the $Q^2$ - $\nu$ plane for $E_0$ = 200 GeV using 18 ft target, for apparatus of E-26 (scale invariant configuration).

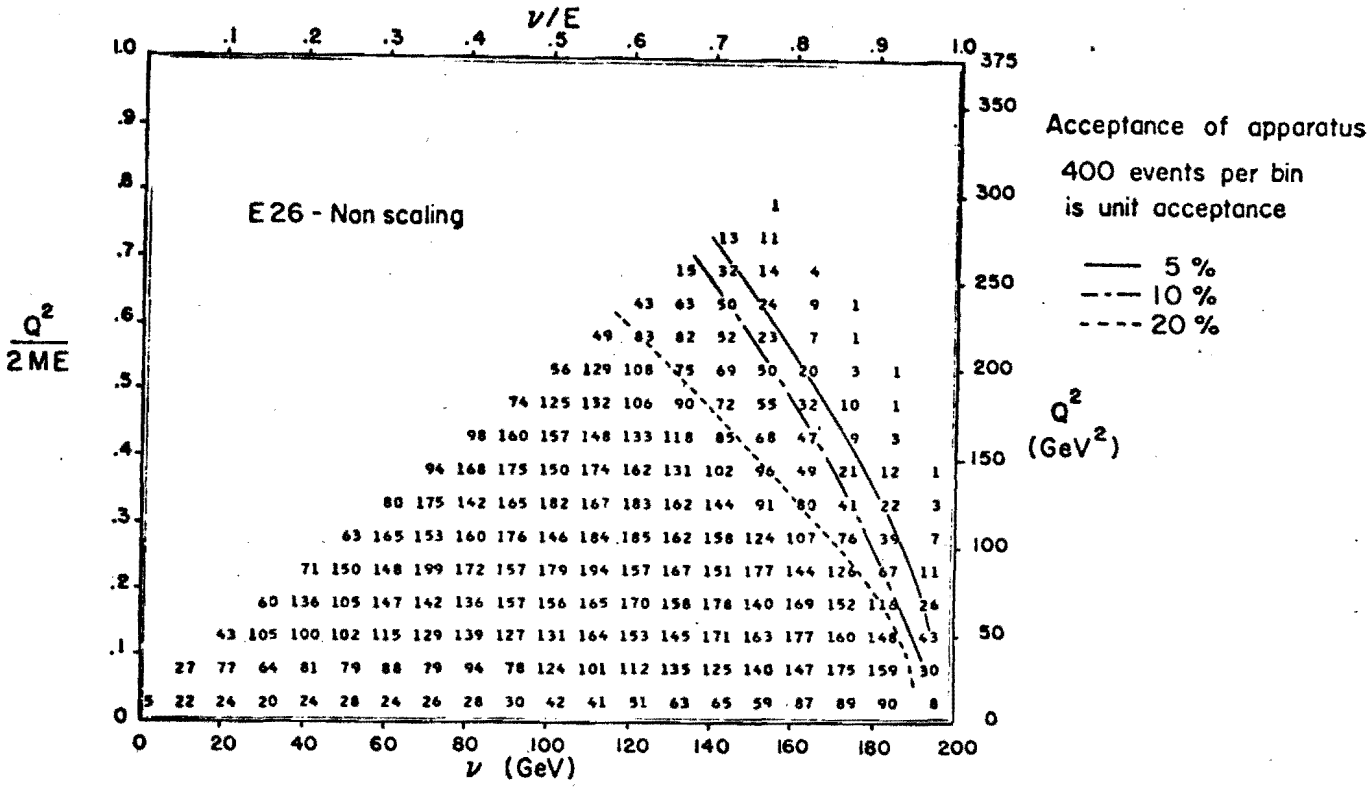


FIGURE 6c. Detection efficiency contours in the $Q^2$ - ν plane for $E_0$ = 200 GeV using 18 ft target, for apparatus of E-26 (non-scale invariant configuration).

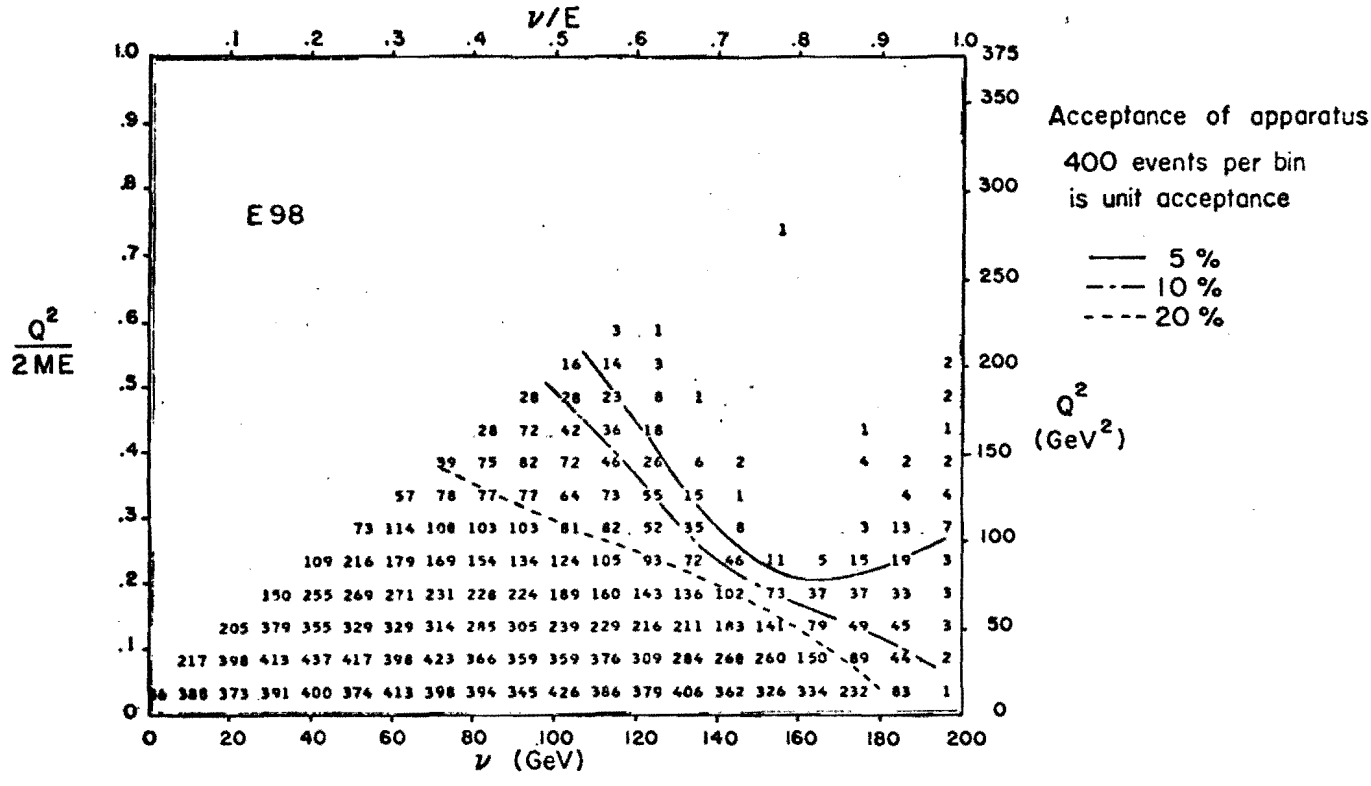


FIGURE 6d. Detection efficiency contours in the $Q^2$ - ν plane for $E_0$ = 200 GeV using 18 ft target, for apparatus of E-98 (normal magnet polarity).

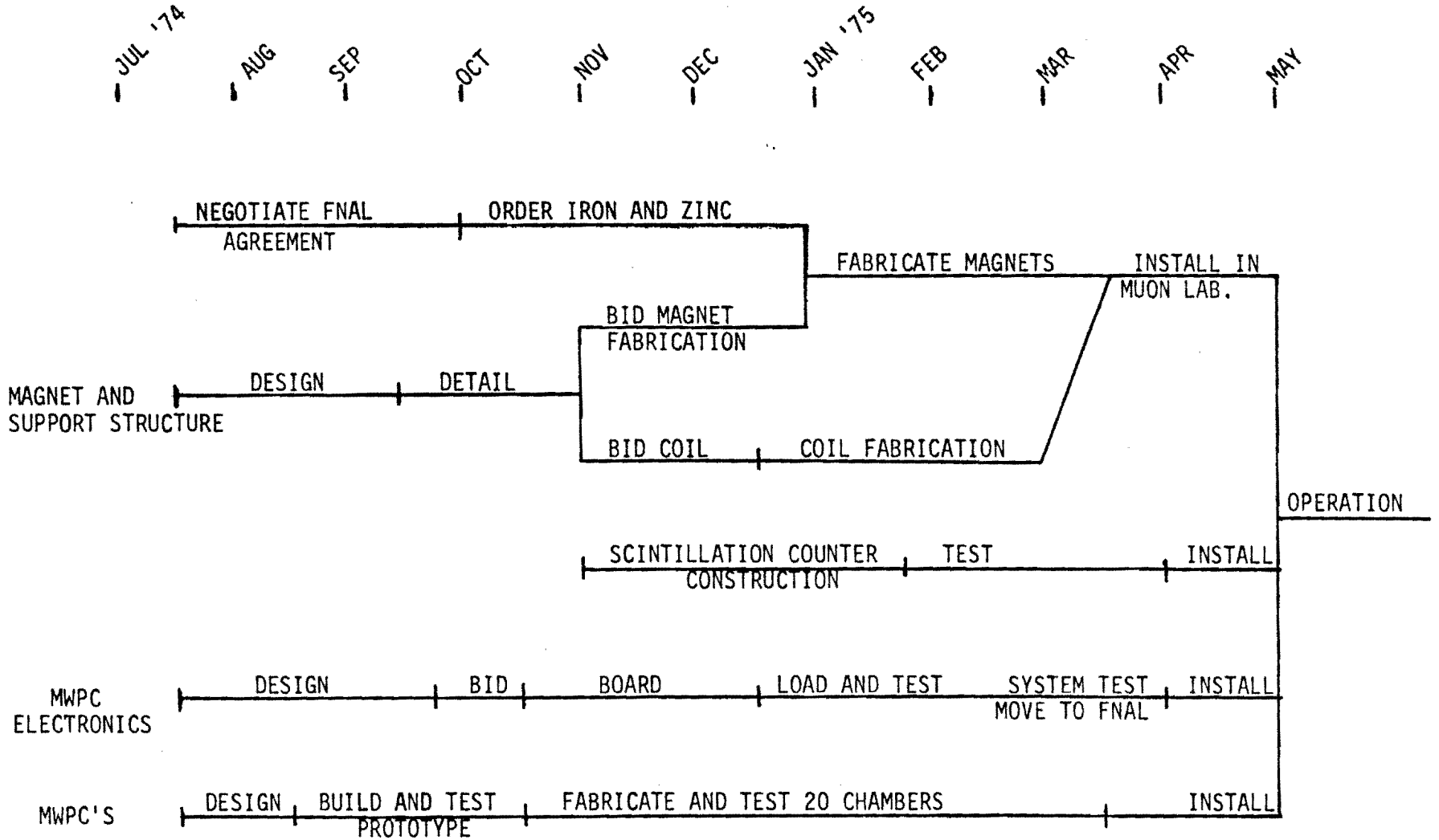


Figure 7. DESIGN AND FABRICATION SCHEDULE

## APPENDIX A - ACHIEVING A SCALE-INVARIANT APPARATUS

In the limit that $\cos\theta \to 1$, the differential cross-section for $\mu N$ scattering can be written

$$\frac{d^2\sigma}{dvd(\ln y)} = \frac{4\pi\alpha^2}{2ME_0}\frac{\nu W_2(\omega,Q^2)}{v^2}\left(1-y+\frac{y^2}{2(1+R)}\right),$$

where

$$v = Q^2/2ME_0$$
$$y = \nu/E_0$$
$$\omega = y/v$$
$$R = \sigma_L/\sigma_T$$
$$M = \text{proton mass.}$$

Clearly, if $\nu W_2$ and R are functions only of $\omega$ the differential cross-section is invariant to transformation of the energy scale, except for the factor $1/E_0$.

A "scale-invariant apparatus" is varied with $E_0$ such that, if $\nu W_2$ and R scale, the accepted, reconstructed events populate the v-y plane in a way independent of $E_0$. The prescription is the following (let the beam direction be $\hat{\zeta}$ and transverse directions be $\hat{\xi}$ and $\hat{\eta}$ ).

(1) To preserve interaction probabilities, the integrated mass density $\int\rho(\xi,\eta,\zeta)\,d\zeta$ is proportional to $E_0$.

(2) For convenience, $\xi$ and $\eta$ apertures and measuring errors are fixed.

(3) Since $v \simeq E'\theta^2/2M$ is scale invariant, $\theta$ for a particular v and y varies as $E_0^{-\frac{1}{2}}$. So, to preserve angular acceptance, the apparatus length $\Delta\zeta$ is proportional to $E_0^{\frac{1}{2}}$. It follows immediately from (1) that the average mass density $\langle\rho(\xi,\eta,\zeta)\rangle \propto E_0^{\frac{1}{2}}$.

(4) The transverse momentum of a scattered muon, $p_\perp \simeq E'\theta$, varies as $E_0^{\frac{1}{2}}$ for fixed v and y. We wish the magnetic field integral to vary the same way, e. g.

$$\int B_{\xi,\eta}(\xi,\eta,\zeta)d\zeta \propto E_0^{\frac{1}{2}}$$

or $$\langle B_{\xi,\eta}(\xi,\eta,\zeta)\rangle = \text{constant.}$$

To summarize, transverse apertures and average magnetic field are fixed, while lengths along the beam direction and average mass densities vary as $E_0^{\frac{1}{2}}$.

It should be noted that, in addition to deep inelastic μN scattering, elastic electromagnetic scattering with constant form factors is scale-invariant. Hence effects due to μ-e straggling and multiple Coulomb scattering also scale in this type of apparatus. Of course, a host of minor phenomena ( Molière scattering, coherent effects in muon dE/dx, internal and external bremsstrahlung, direct pair production ) involve non-pointlike form factors or multiple-photon exchange and produce scale-noninvariant effects. A discussion of the scaling performance of the proposed apparatus is contained in the main text.

## APPENDIX B - MAGNET CONSTRUCTION

The precision required of the iron slabs is such that shaping by flame-cutting is adequate. The requirements on the magnetic properties would allow them to be fabricated from reject low-carbon steel plate, available from mills near FNAL. The winding slots, as well as the outside edges, are flame-cut. After all 72 4-inch slabs are arranged in the Muon Laboratory, they are tack-welded to longitudinal channels for support, and a single coil is wound through all the slots. There are thus only two places where the coil is transverse to the beam, resulting in a large reduction in the total length of the winding.

With the dimensions shown in Fig. B1 a field of 19 kG is reached with 50,000 ampere turns. Since the width of a coil window adds little to the amount of iron, it seems natural to choose aluminum conductors. A possible choice would be rectangular aluminum bars, 3/4 in high by 1-1/2 in wide, with a 1/2-in diameter water cooling hole. The winding slots would then accommodate 50 turns in a single stack with the result that the current could be 1000 amperes. The total resistance would be 84 milliohms and the power 84 kW. The total weight of conductor, with these dimensions, is 6300 lbs. Without good figures on unit costs, one cannot estimate closely, but this choice of dimensions appears to give a reasonable balance between the cost of the coil and the cost of the power supply. Of course, these preliminary conductor dimensions can be adjusted to properly match available power supplies, or to optimize the total cost of power supplies and windings.

We imagine that the coil bars would be insulated with epoxy impregna-

ted glass sleeving cured in advance of winding, and that the bars would then be inserted into the slots. The water connections would be aluminum hose bibs welded on in advance. The cross-connections at the ends could either be welded in the field or clamped. The soft aluminum bars with these dimensions would be easily bent after installation to provide space to make the connections. It should be noted that the magnetic forces on the conductors are negligible in a magnet such as this without airgap. There is nothing to be gained by compact end connections. Insulation of the cross-connections at the ends of the spectrometer can be easily and adequately done in the field.

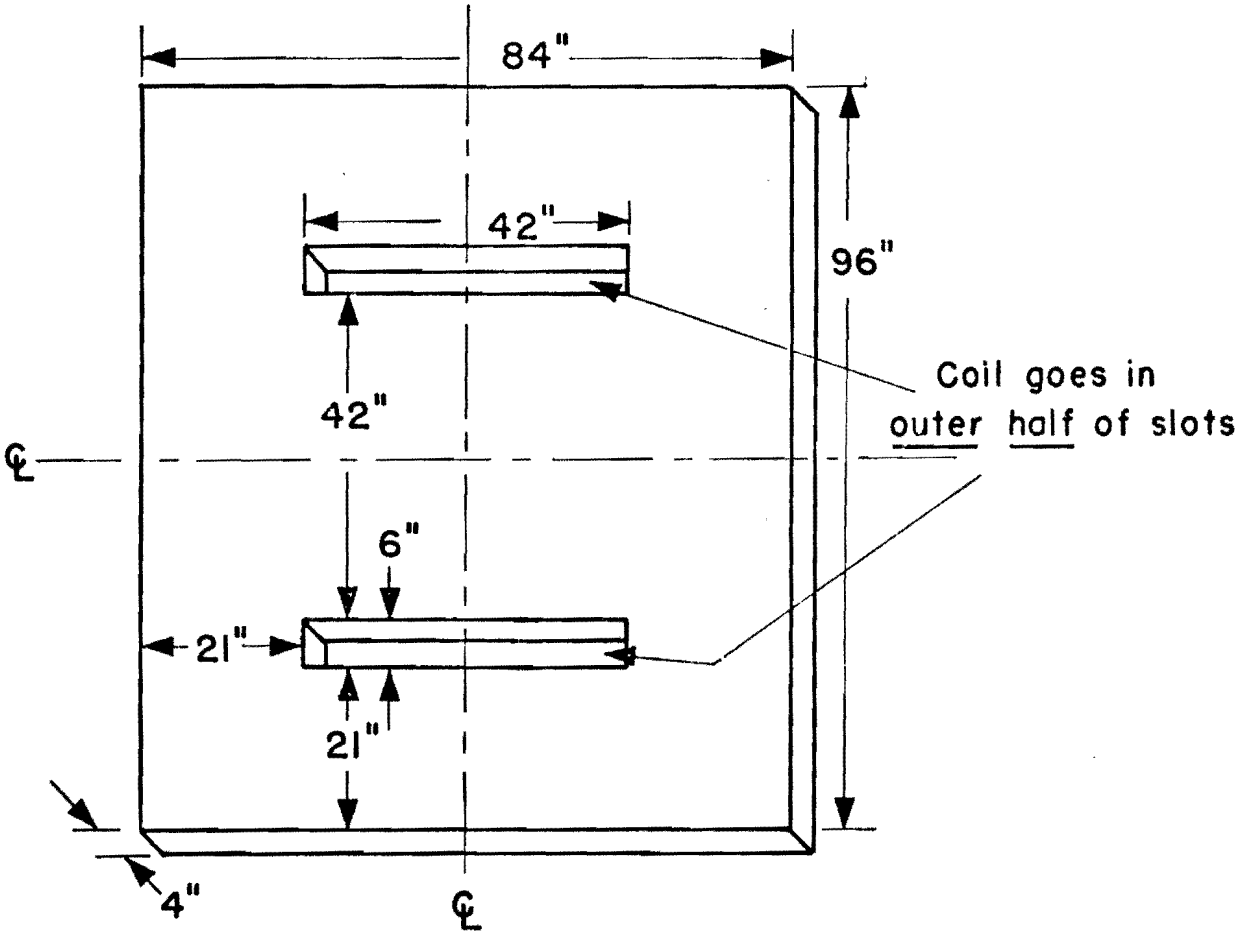


Notes:

1) Dimensions in inches.
2) All edges flame-cut ± 1/8 inch.
3) Coil - 50,000 Ampere-turns.
4) Carbon content of steel: 1010 or less.
5) Plate flatness ± 1/4 inch.



FIGURE B1.

## APPENDIX C - CALORIMETER CONSIDERATIONS

### Calorimeter Fundamentals

Although we are constrained to use iron in the calorimeter considered here because of its magnetic properties, it should be noted that iron is an excellent material for a calorimeter composed of scintillators sandwiched between slabs of converters. That is, the nuclear absorption length in iron is sufficiently short that nuclear cascades will be contained in a relatively small volume ( ~ 1 meter in the longitudinal direction for energies considered here). And a radiation length in iron is sufficiently long that even with relatively coarse sampling of the hadronic cascade, photon showers from produced $\pi^0$'s will be sampled in a representative manner.

As an illustration of this last point, consider two sampling calorimeters, one made of a lead-scintillator sandwich and the other of iron and scintillator. Further, suppose the scintillators in each calorimeter are separated by 1/2 absorption lengths (8.6 cm vs. 9.1 cm) of the converter. In the lead sandwich this corresponds to $\gtrsim$ 16 r.l. while in the iron case the separation corresponds to $\lesssim$ 4.8 r.l. Photons produced from $\pi^0$'s in the lead will clearly not be sampled as uniformly as if they had been produced in the iron sandwich. Indeed, in the lead case there is a fair probability that the shower from the $\pi^0$ could be absorbed entirely in the lead with little or no ionization picked up by the scintillator.

In fact, it is the probability that the $\pi^0$'s will be sampled properly over their subsequent electromagnetic cascades which determines the energy resolution of a sampling calorimeter. Thus, at a given incident

energy, the error in the energy measurement is a function of the thickness of the converter.

Of course, particles other than $\pi^0$'s play a role in the energy resolution of a sampling calorimeter. The amount of ionization picked up by the scintillators due to particles other than $\pi^0$'s is proportional to the total number of these particles in the hadronic cascade. To a good approximation the number (N) of these hadrons is proportional to the energy of the incident particle(s), $N \sim E$. Assuming a statistical fluctuation in N of $\sqrt{N}$ leads to the conclusion that the energy resolution of a calorimeter goes as

$$\sigma_E \sim \sigma_N \sim \frac{1}{\sqrt{N}} \sim \frac{1}{\sqrt{E}} .$$

Luckily, since iron is a particularly good material for sampling calorimeters, devices of the iron-scintillator type have been studied extensively using Monte Carlo methods,[1] prototype models[2] and detectors in actual experiments.[3] Consequently, in deciding the basic parameters to be used in the μ-N calorimeter, we have been able to rely to a great extent on the collected wisdom of those who have gone before us. One particular exception to this, where we have tried to add some fresh information, concerns the transverse development of hadronic cascades and the question of particle leakage out of the sides of a rectangular calorimeter. In this case we have used data from a large steel-scintillator detector[4] which was built at Serpukhov to study high energy photons in a $\pi^- p \to \pi^0 n$ experiment.

In the following we discuss a) the size of the calorimeter scintilla-

tors necesssary to contain the hadronic cascade, b) the thickness of the steel plates necessary to give a particular energy resolution, and the possibility of making a calorimeter which can be "scaled" to have the same energy resolution at two different incident muon energies, c) the shape and construction of the scintillation counters with emphasis on the versatility necessary to do other experiments, and d) the characteristics of the ADCs and problems with and methods of the calibration and monitoring of the calorimeter counters.

Scintillator Size

The Serpukhov detector, shown schematically in Fig. C1, is only 20 r.l. deep and so the entire hadronic cascade is rarely entirely contained for incident hadrons of interest. Each scintillator, however, is actually a system of 64,1.5 cm wide hodoscope staves each of which has its own ADC. Thus the hadronic shower profile can be measured at four sequential positions in the shower's development. We have looked at cascades produced by 40 GeV $\pi^-$ and have measured the average amount of energy beyond some projected distance , from the shower axis. The results and an idealization of the experiment are shown in Fig. C2. The interaction point was chosen to be at the start of the detector by demanding that the first block in the detector have more than 1 minimum ionizing particle in it.

The fraction of energy lost out of the end of the detector was determined from the Monte Carlo results of W. V. Jones. Thus it can be seen that if the hadron cascade is 2" inside the edge of a calorimeter with rectangular cross section, ~ 10% of the ionization energy will leak out

the side. This assumes that the tail of the cascade which was not seen because the detector was too shallow would have the same profile as the last measured profile.

Based on these studies we conclude that for a hadronic cascade with its axis parallel to and more than 2-1/2 inches inside the edge of a rectangular Fe-scintillator calorimeter a negligible degradation of energy resolution will occur due to leakage out the side.

But, the axis of the hadronic cascade in $\mu$ -N scattering will not be parallel to the axis of the calorimeter. In fact the cascade direction will depend on the kinematic variables $q^2$ and $\nu$. Fortunately, the expected length of a hadronic cascade only weakly depends on the cascade energy. In the interval between 20 and 200 GeV the expected cascade length in iron is about 1 m and increases by about 30% over the interval. Nevertheless, the particular incident energy and trigger conditions will have to be considered to decide the minimum separation between the incident muon trajectory and the calorimeter scintillator edges which are opposite the scattered muon; something between 6" and 8" may be desirable.

The total cross-sectional area of each of the scintillation counters will depend on the size of the useful muon beam.

Plate Thickness.

In the experiment to measure scaling in deep inelastic muon-proton scattering the calorimeter scintillators will be used to determine the interaction vertex. Calculations have shown that 4" steel plates between the scintillators will be sufficiently thin for this purpose.

Because of the fluctuations in the sampling of $\pi^0$ - induced showers,

as mentioned above, the energy resolution of the calorimeter as a function of plate thickness is rather difficult to calculate except by Monte Carlo methods. Fig.C3 shows the expected energy resolution of the calorimeter ($\nu = E_{hadrons}$) for plate thicknesses of 2" and 4" as derived from the Monte Carlo results of Baroncelli. Also shown in this figure is the expected $\nu$ resolution using only the measured energy of the scattered muon ($\nu = E_0 - E'$). As can be seen, $\nu$ is best measured at large $\nu$ by this method while it is measured best at smaller $\nu$ by means of the calorimeter.

For convenience, the expected resolutions are plotted for the two "scaling" energies 200 GeV and 4/9(200) = 89 GeV. The resolution in $\nu$ as determined from the scattered muon is constant as a function of the normalized abscissa $y = \nu/E_0$; this is because $\Delta p/p \sim 13\%$ is determined by multiple scattering in the iron and extra material has been put into the spectrometer to keep the fractional momentum resolution a constant for both incident energies.

The $\nu$ resolution of the spectrometer for a fixed plate thickness depends only on the energy of the shower. Thus, if one used a calorimeter with 4" plates, the resolution in $\nu$ for $y < .5$ would be different by a factor of more than 1.15 for the two incident muon energies. That is, the apparatus doesn't scale if the calorimeter is used to determine $\nu$.

As is quickly seen from Fig.C3, there is the possibility of making a "scale invariant" calorimeter. The resolution in $\nu$ for 4" plates at $E_0 = 200$ GeV is almost the same as for 2" plates at $E_0 = 89$ GeV. To scale the apparatus it is only necessary to ignore the information from every other scintillator when running at 200 GeV. The 4" numbers require some extrapolation from Baroncelli's Monte Carlo and some additional work is indicated to make sure all is as it seems.

The relevance of the $\nu$ resolution can be easily demonstrated. There is the possibility of trying to compare our results with other experiments done at lower energies at SLAC and other places. In this case we see that

$$\left(\frac{\Delta Q^2}{Q^2}\right)^2 \simeq \left(\frac{\Delta E'}{E'}\right)^2 + \left(\frac{\Delta\theta^2}{\theta}\right)^2 + \left(\frac{\Delta E_0}{E_0}\right)^2 \simeq 13\%$$

and

$$\left(\frac{\Delta\omega}{\omega}\right)^2 \simeq \left(\frac{\Delta Q^2}{Q^2}\right)^2 + \left(\frac{\Delta\nu}{\nu}\right)^2 + \text{correlation, if applicable}$$

$$\simeq (.13)^2 + \left(\frac{\Delta\nu}{\nu}\right)^2 .$$

Whenever $\nu \lesssim 0.5E_0$, $\nu$ is the determining error in $\omega$. To compare with absolute measurements at lower energies, we should try to do as well as possible in measuring $\nu$. The nuclear Fermi motion leads to an intrinsic $\Delta\nu/\nu$ resolution of about 12% for $\mu$-N interactions, however.

Baroncelli's Monte Carlo calculation of $\Delta\nu/\nu$ indicates that at 20 GeV 1", 2", 3" plates are 2%, 9%, 36%, resp. worse than infinitesimally thin plates. At 100 GeV the numbers are 2%, 8%, 20% resp. The extrapolated values for 4" seem to give $\Delta\nu/\nu$ between 90% and 50% worse than the ideal calorimeter. This disagrees slightly with the Monte Carlo results reported in the proposal of experiment E-21 where it was concluded that 4" was about 30% worse than 2".

As a final remark on the subject of converter thickness, it must be noted that little or no information is obtained by studying the shape of the cascade's longitudinal development. Unlike electromagnetic showers, because the fluctuations in the hadron cascade are so great, the maximum amount of information to determine the initial hadron energy is obtained by summing the pulse heights in the calorimeter counters.

## Scintillator Construction

Because the expected muon beam is limited in size and because the transverse development of the hadron cascades is also limited, the size of the calorimeter scintillation counters can be less than 2' on a side. For this reason and the fact that a large amount of plastic scintillator is available we have not considered anything but conventional plastic scintillators with simple light pipes.

The two major considerations in the scintillation counter design are 1) the uniformity of response of the counter for showers distributed over the face of the counter and 2) the requirement that the counters be moveable to the extent that they can be used in other positions relative to the iron core magnets to allow other experiments such as Experimental Proposal 203A. Long light pipes, necessary in any case to get the photomultipliers out beyond the iron of the magnet blocks, are useful for both considerations. It will also be possible to look at each scintillator with two photomultipliers on opposite sides and add the signals to make the response more uniform. On the other hand, since the position of the shower is known from the proportional counter information, it will be easy to apply a correction factor for any nonuniformity of response.

## Calorimeter Calibration

Because of the non-linear response of the calorimeter to initial hadron energies, it is desirable to have methods of calibration over the entire range of energies to be used in the experiment. The amount of shower energy which excites nuclear states in the iron and is not seen in the scintillator can be expected to change from 40% to 30% as the hadron shower

energy changes from 20 to 200 GeV. Other effects due to scintillator, photomultiplier and ADC non-linearities are expected to be negligibly small.

As can be seen from Fig.C3, for hadron cascades of energy greater than about half the incident muon energy the calorimeter can be easily calibrated by demanding the internal consistency of μ-N scattering events. These events also allow a method for monitoring the performance of the calorimeter during the course of the experiment. However, to measure the response of the calorimeter at low energies it would be advantageous to have an incident muon beam of lower momentum.

To our knowledge, no one has ever used magnetized iron in an iron-scintillator sampling calorimeter. The effects expected in the cascade or shower development due to the magnetization are expected to be small, but they should be measured directly, if possible. The "dummy" blocks (e.g., Zinc) used to make the apparatus scale invariant for two different energies will also be used as calorimeter converters and could conceivably cause a difference in the calorimeter's energy resolution. This also argues for an in situ calibration study.

The number of minimum ionizing particles at the maximum of a hadronic cascade is expected to be $\sim$ 0.5/GeV. (An electromagnetic shower in a similar iron-scintillator calorimeter will give about 3 minimum ionizing particles/GeV at the shower maximum.) Thus a 200 GeV cascade gives $\sim$100 minimum ionizing particles at cascade maximum on the average. Also, the statistical fluctuations are enormous ($\sim$70% at cascade maximum). Consequently, if the beam muons are to be used to constantly monitor the scintillator performance, the range of the ADCs must be large enought to see average

variations in single particle pulse height while being able to see showers 200 times bigger without saturation. Further, if there is any non-uniformity of response over the face of the scintillators the ADC range must be correspondingly enlarged. The desired ADC range (in bits of output), given the prerequisites mentioned above, will depend somewhat on the pedestal stability of the chosen ADC.

## References


1. W. V. Jones, P. R. D1, 2201 (1970).
   A. Baroncelli, "Study of total absorption counters for very high energy particles". Instituto Superiore Di Sanita, Rome Preprint ISS P73/8 (Sept. 1973).
   T. A. Gabriel and K. C. Chandler, Particle Accelerators 5, 161 (1973).
   See also the FNAL E-21 experimental proposal for both Monte Carlo and prototype results.

2. W. J. Willis and V. Radeka, "Liquid Argon Ionization Chambers As Total Absorption Detectors", BNL 18813 (April 1974), submitted to Nucl. Instr. and Meth.

3. J. Engler, W. Flauger, B. Gibbard, F. Monnig, K. Runge and H. Schopper, Nucl. Instr. and Meth. 106, 189 (1973).

4. Yu. B. Bushnin, S. V. Donskov, A. V. Inyakin, Rolland P. Johnson, V. A. Kachanov, S. V. Klimenko, R. N. Krasnokutsky, A. A. Lebedev, A. A. Lednev, Yu. V. Mikhailov, Yu. D. Prokoshkin , E. A. Razuvaev, R. S. Shuvalov, "A Hodoscope Spectrometer For High Energy Photons", IHEP Preprint (1974), submitted to Nucl. Instr. and Meth. Also described in the CERN COURIER 3, 83 (March 1974).

SERPUKHOV PHOTON DETECTOR USED TO MEASURE
HADRON CASCADE WIDTHS

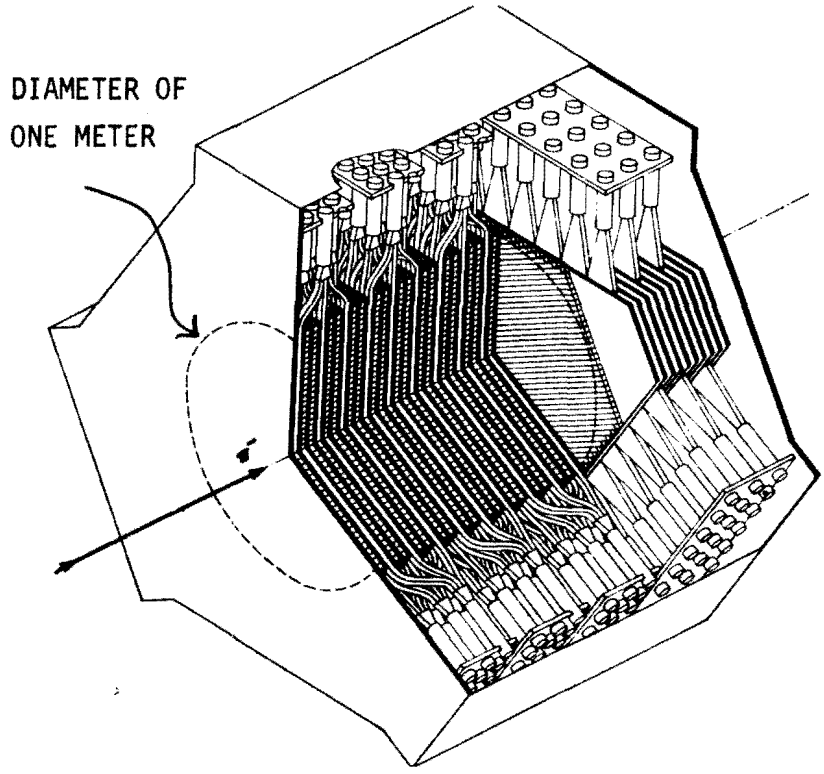


*Diagram of the gamma detector showing how it is built up of alternate sheets of 1 cm steel and scintillator. The photomultiplier tubes are arranged around the outside.*

FIGURE C1

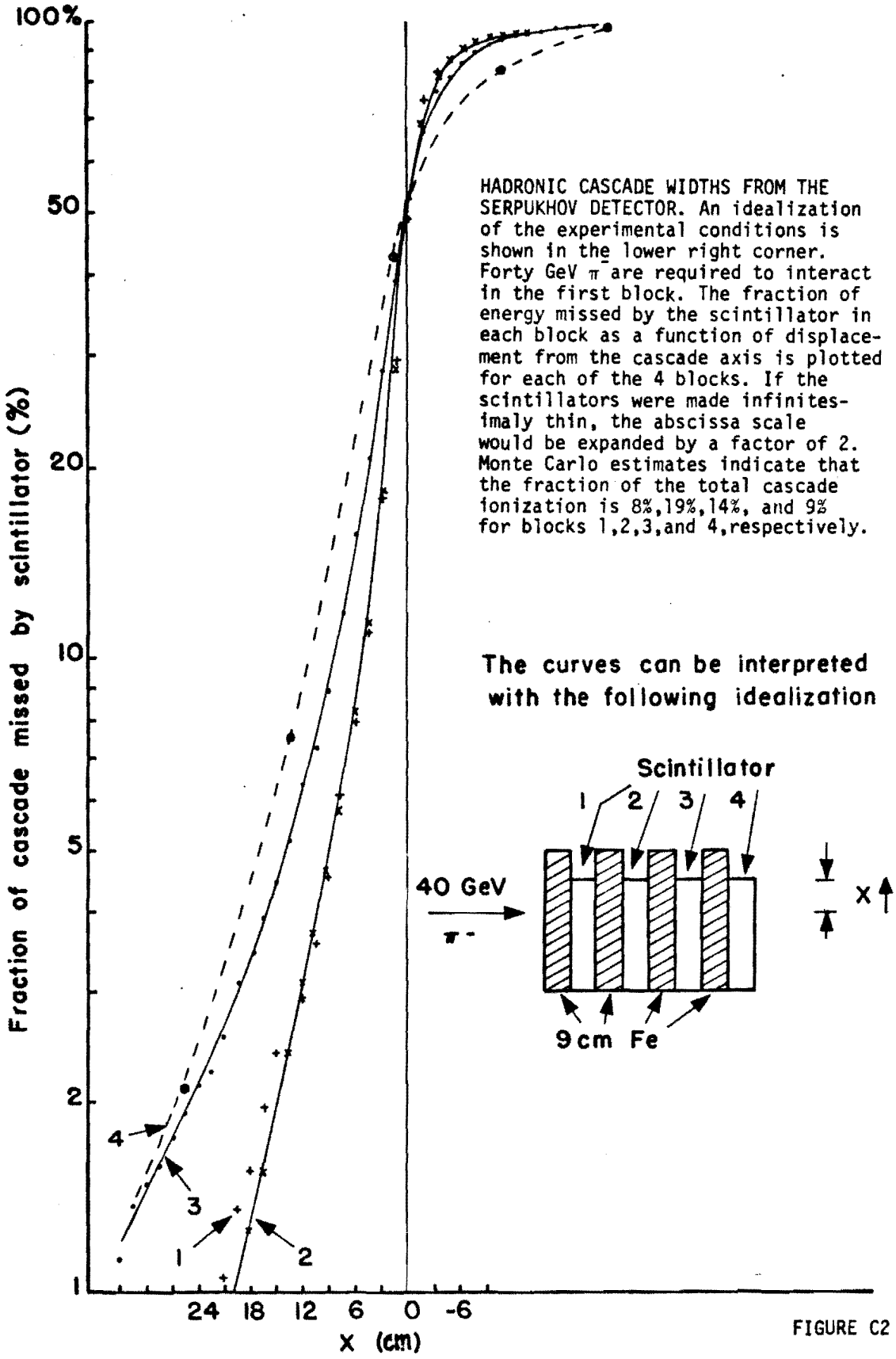
100%
50
20
10
5
2
1
Fraction of cascade missed by scintillator (%)
24 18 12 6 0 -6
X (cm)
4
3
1
2
HADRONIC CASCADE WIDTHS FROM THE SERPUKHOV DETECTOR. An idealization of the experimental conditions is shown in the lower right corner. Forty GeV π⁻ are required to interact in the first block. The fraction of energy missed by the scintillator in each block as a function of displacement from the cascade axis is plotted for each of the 4 blocks. If the scintillators were made infinitesimaly thin, the abscissa scale would be expanded by a factor of 2. Monte Carlo estimates indicate that the fraction of the total cascade ionization is 8%,19%,14%, and 9% for blocks 1,2,3,and 4,respectively.
The curves can be interpreted with the following idealization
Scintillator
1 2 3 4
40 GeV
π⁻
X
9cm Fe

FIGURE C2

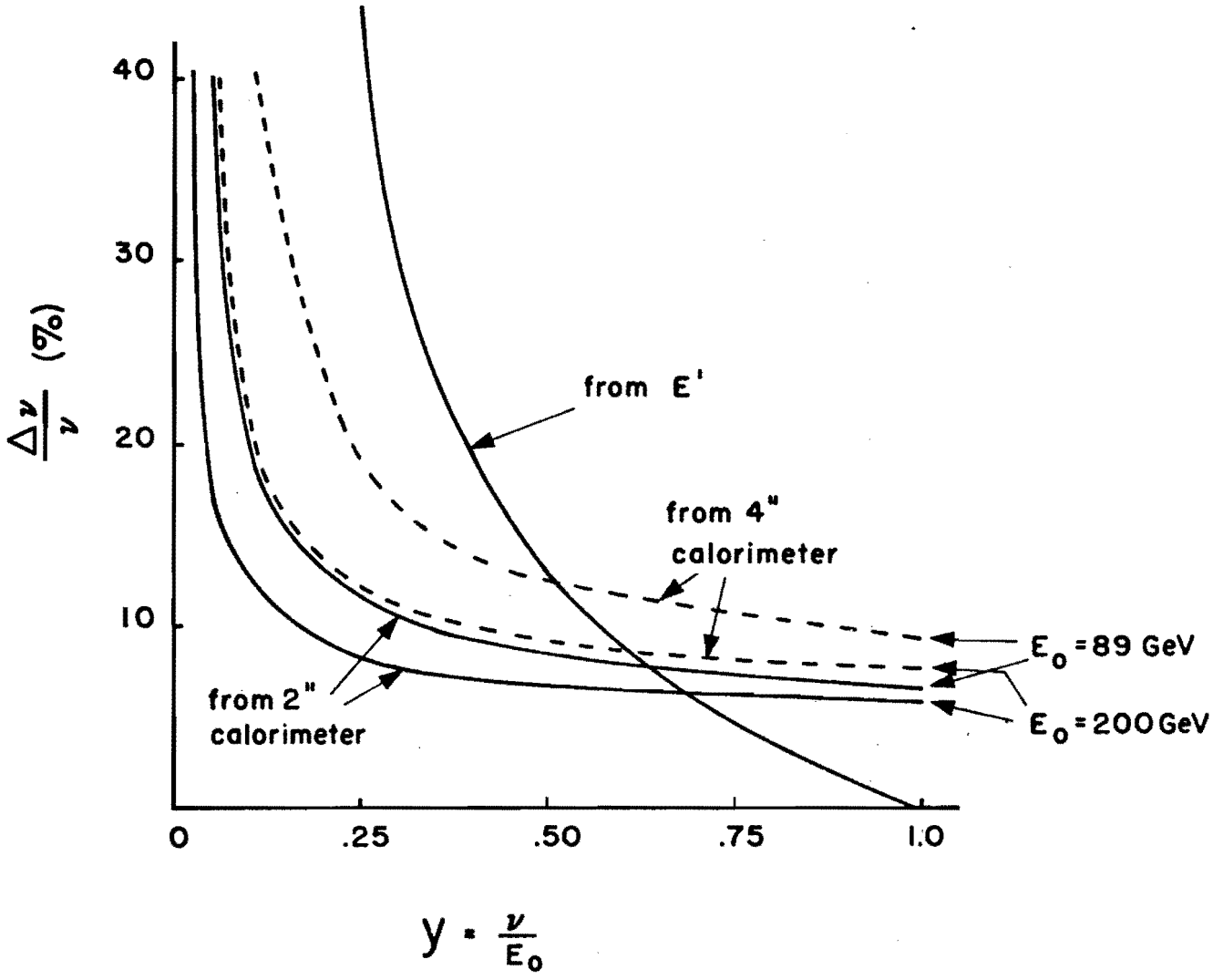


FIGURE C3 COMPARISONS OF SOURCES OF UNCERTAINTY IN $\nu$. Baroncelli's Monte Carlo has been used to determine the error in $\nu$ due to the calorimeter resolution for 2" and 4" iron plates. The results have been plotted for the two scaling energies, 89 and 200 GeV. Also shown is the error in $\nu$ determined by the momentum analysis, $\nu = E_0 - E'$. The contribution to the uncertainty in due to the Fermi motion in the iron nucleus is expected to be 12%.

## APPENDIX D - ASSUMPTIONS FOR ACCEPTANCE CALCULATIONS

Recorded here are the assumptions used for calculation of the acceptances shown in Figs. 5 and 6. In all cases, scaling, $E_0$ = 200 GeV, and the SLAC value for $\nu W_2$ have been used. Only those apparatus dimensions important in determining acceptance are listed. We use a coordinate system in which the beam direction is $\hat{z}$, $\hat{x}$ is up, and the target is centered at z = 0. The beam (50 $in^2$ area) is centered at x = y = 0. Dimensions are in inches.

This proposal.

Maximum $Q^2$ set by ($-9 < x < 33$, $-3 < y < 48$ at $z = 346.5$).
Minimum $Q^2$ set mostly by ($y > 6$ at $z = 274.5$), but this is expected to change as trigger counter geometry is finalized.
Magnetic field: Bending direction is $-\hat{x}$,
Extent is from interaction to $z = 346.5$,
Average $p_\perp$ is 2.14 GeV/c.

Experiment 26 (scaling configuration).

(a) 18 foot iron target.
Maximum $Q^2$ set by ($r < 36$ at $z = 591$).
Minimum $Q^2$ set by ($r > 6$ at $z = 159.5$ and $z = 496.5$).
Magnetic field: Bending direction is $-\hat{r}$,
Extent is $159.5 < z < 496.5$,
$p_\perp$ is 2.14 GeV/c.

(b) 3 foot iron target.
Same as above except all z's smaller by 161.5.

Note that this is the same 8-magnet configuration which has been used by E-26, except that the target position has been near-optimized for high $Q^2$ in each case. Also, it has been assumed that the trigger counters fully cover the magnet annulus, which is not the actual case.

Experiment 26 (nonscaling configuration).

(a) 18 foot iron target.
Maximum $Q^2$ set by ($r < 36$ at $z = 325$).
Minimum $Q^2$ set by ($r > 6$ at $z = 158.5$ and $z = 273.5$).
Magnetic field: Bending direction is $-\hat{r}$ ,
Extent is $158.5 < z < 273.5$,
$p_\perp$ is 1.28 GeV/c.

(b) 3 foot iron target.
Same as above except all z's smaller by 53.5.

This is a possible arrangement of E-26 in the 3-magnet configuration, designed to minimize the apparatus length and near-optimize the target position at high $Q^2$.

Experiment 98.

(a) Normal polarity.
Maximum $Q^2$ set by ($|x| < 39.5$, $-42.5 < y < 115.5$ at $z = 976$).
Minimum $Q^2$ set by trigger criterion, which is assumed (because of our ignorance) to eliminate no events.
Magnetic field: Bending direction is $\hat{y}$ ,
Impulse of $p_\perp = 2$ GeV/c at $z = 186$.

(b) Reversed polarity.
Same as above except bending direction is $-\hat{y}$ .

These apertures were taken from Fig. IV.1 of the E-98 Status Report (Sept. 14, 1972), except that the apparatus was reflected about the xz plane to correspond to its current deployment. All apertures were assumed to be infinite except that of the most downstream spark chamber. The (fictitious) 18-foot iron target was placed in available space just upstream of the magnet; in this calculation, the acceptance is insensitive to its exact position.

Proposal 307
Correspondent: L.T. Kerth
FTS/Com 415 843-2740 Ext. 5501

Addendum

# MUON-NUCLEON SCATTERING WITH EXTRAORDINARY MOMENTUM TRANSFER

A.R. Clark, E.S. Groves, L.T. Kerth, S.C. Loken, M. Strovink, W.A. Wenzel

Department of Physics and Lawrence Berkeley Laboratory,
University of California, Berkeley, California 97420

Rolland P. Johnson
Fermi National Accelerator Laboratory, Batavia, Ill. 60510

F.C. Shoemaker
Joseph Henry Laboratories, Princeton University,
Princeton, N.J. 08540

December 13, 1974

Introduction

Since submitting proposal 307 we have continued to investigate the acceptance of the proposed apparatus. As a consequence of this study we now propose some minor changes in the experiment. We have also done a detailed cost estimate for the construction of the magnet. We present here these considerations.

Event Trigger

Our study has shown that an improvement in the "scale invariance" of the apparatus can be achieved by placing trigger counters in each of the modules (M7 through M18) of the spectrometer (see figure 2 page 33 of the proposal). This matches the trigger granularity to that of the physical construction of the spectrometer. The change represents a minor increase in cost and complexity that is warranted to further reduce systematic effects in the test of scaling.

Spectrometer Acceptance

We have carried out a more detailed Monte Carlo simulation of the apparatus and have calculated the acceptance for beam energies of 200 GeV and 240 GeV. Any experiment of this type benefits from operation at the highest possible beam energy consistent with adequate particle flux. We had assumed an energy of 200 GeV as an example in the original proposal. The acceptance calculation at 240 GeV provides a comparison with other proposals. It is our present understanding that adequate flux can be obtained up to 225 GeV but not at 240. Thus, it is probable that 225 GeV will be the final choice for any experiment.

The results of our acceptance calculations are shown in figure A1 a for 200 GeV. This figure should replace figure 6a page 37 of the proposal. Figure A1 b shows the acceptance at 89 GeV in the scaled configuration with the zinc plates of the spectrometer removed. Com-

parison of figures A1 a and A1 b shows the scale invariance of the spectrometer. Figure A2 shows the acceptance of the spectrometer of this proposal at 240 GeV. Figure A3 gives the total acceptance as a function of $Q^2$ for beam energies of 200 and 240 GeV. These show the acceptance of this spectrometer extends well above a $Q^2$ of 200 $(GeV/c)^2$.

It is clear that the more detailed studies of scaling proposed for a second generation experiment must provide good coverage in all kinematic variables. Figure A4 shows the acceptance of the proposed apparatus as a function of both $Q^2$ and the Bjorken scaling variable x. The experiment covers most of the kinematic region and will allow comparison with many proposed models of scaling violation.

These studies have supported our previous work. The spectrometer has good acceptance at $Q^2$ above 200 $(GeV/c)^2$, and is scale invariant to high order.

Magnet Cost Estimate

We have asked the engineering group at Berkeley to make an independent cost estimate for the magnet (appendix AA). This estimate has been made from a conservative point of view. We have tried to include everything and have made no assumption regarding the possibility of sources of cheap labor or materials. Therefore, we believe it is an absolute upper limit. We comment on each item to indicate where possible savings can be made.

1) Magnet Steel - The estimate for material assumes new steel must be obtained and it is based on the quote of only one supplier. We would at the time of approval of the proposal immediately try to find distressed steel of approximately 4". If it should be available it might reduce the cost of

the plates by a large factor. There is no way that we can estimate this at the moment. It is our understanding that Fermilab does not have plates as thin as 4 inches in its stock.

2) Aluminum Conductors - Since there are only a limited number of suppliers for this material this estimate is based on a quote from one supplier and is probably quite accurate.

3) Coil Fabrication - We are presently rethinking the method of cross connects at the magnet ends. There may be some saving in the way these are designed.

The insulation of the conductors we would expect to do ourselves with our own tape wrapping machine which we would bring to the Fermilab. We are also conducting tests on a new epoxy insulation that can be sprayed on which if it should prove to be mechanically sound would represent considerable savings.

We would expect to do all of the mechanical work on the coil fabrication ourselves with the exception of the welding. These two items we believe would reduce the cost to the Fermilab by $5,000 over that shown.

4) Magnet Assembly Costs - The stacking of the plates and the welding would require the help of some riggers and a welder. We would expect to do the installation of the coil and its pressure checking. We would also do the installation of the tracks for the zinc plates ourselves. This should reduce the cost shown by $2,500.

5) Zinc Plates - This price is an upper limit in that it assumes non-GSA zinc. Our quote from a San Francisco foundry is only for convenience in obtaining a number. We would of course expect to have the plates cast in the Chicago area. It is our understanding that GSA zinc is 35¢ per pound rather than 46¢ quoted by the foundry. This would represent a savings of $8,800.

6) Engineering Design and Drafting - We would expect to pay for this as well as to assume responsibility for the supervision of the vendors (as stated in the original proposal).

7) Hangers and Tracks for Zinc - This cost is mostly material and is thus accurate.

8) Support - The use of concrete piers is the cheapest way to support the magnet. The piers can be broken up and removed at the end of the experiment.

9) Contingency - The contingency is a matter of taste but is certainly conservative. In the following discussion we have not considered contingency.

In all we feel that the most probable cost to NAL for the magnet would be 215K$ with 235K$ as an absolute upper limit.

Magnet Power Supply

We have not estimated the cost of a power supply for the magnet. It operates at 1000 amps at ~85 volts. It can be powered easily by one of the Fermilab's "Anocut" 225 KW supplies. It is our understanding that there are several of these available.

We would design the cross section of the conductor to match whatever power supply is available so as to have a power factor as close to 1 as possible.

Conclusion

The proposed apparatus provides a significant increase in precision for the test of scaling and the data obtained at high $Q^2$ more than justify the modest expenditure. This is particularly inexpensive when one compares it with the large commitment in operating funds required from the Fermilab for any experiment. In this context the cost of the magnet is quite modest and represents therefore the most physics for the dollar.

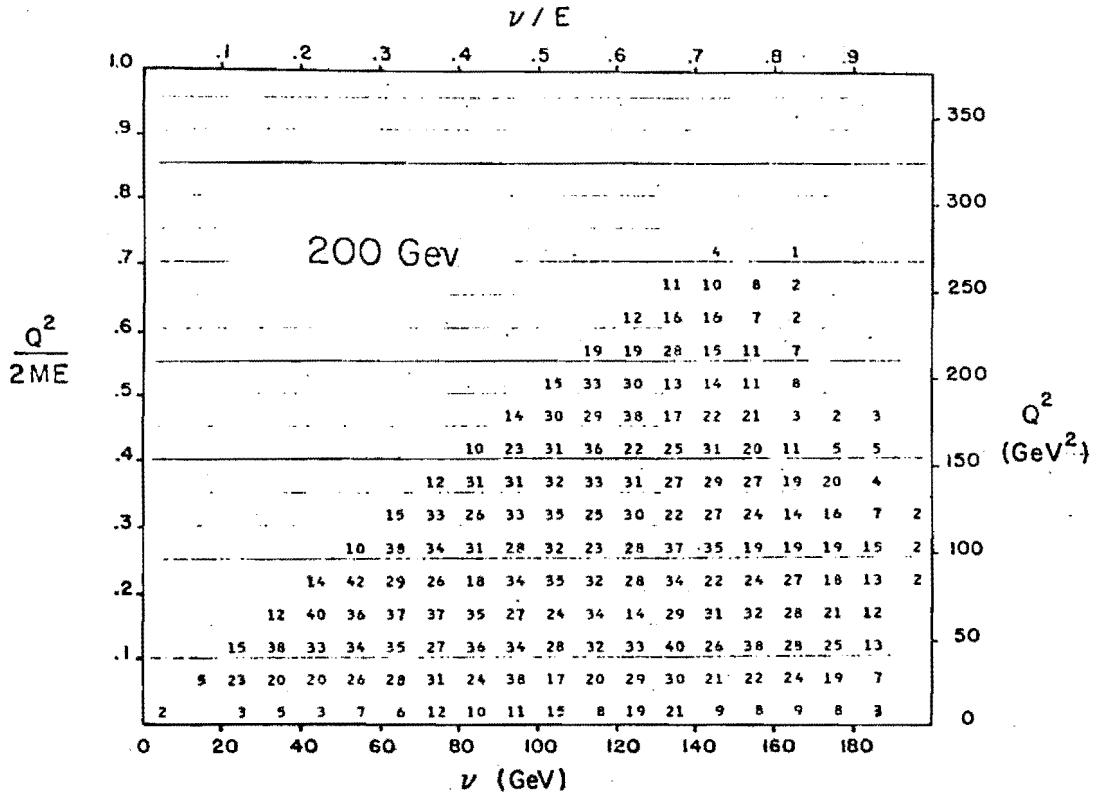


FIGURE A1a. Detection efficiency in the $Q^2$ - $\nu$ plane for $E_o$ = 200 GeV, with the apparatus in the 200-GeV scale-invariant configuration as described in P307. Unit acceptance is 100 events per bin.

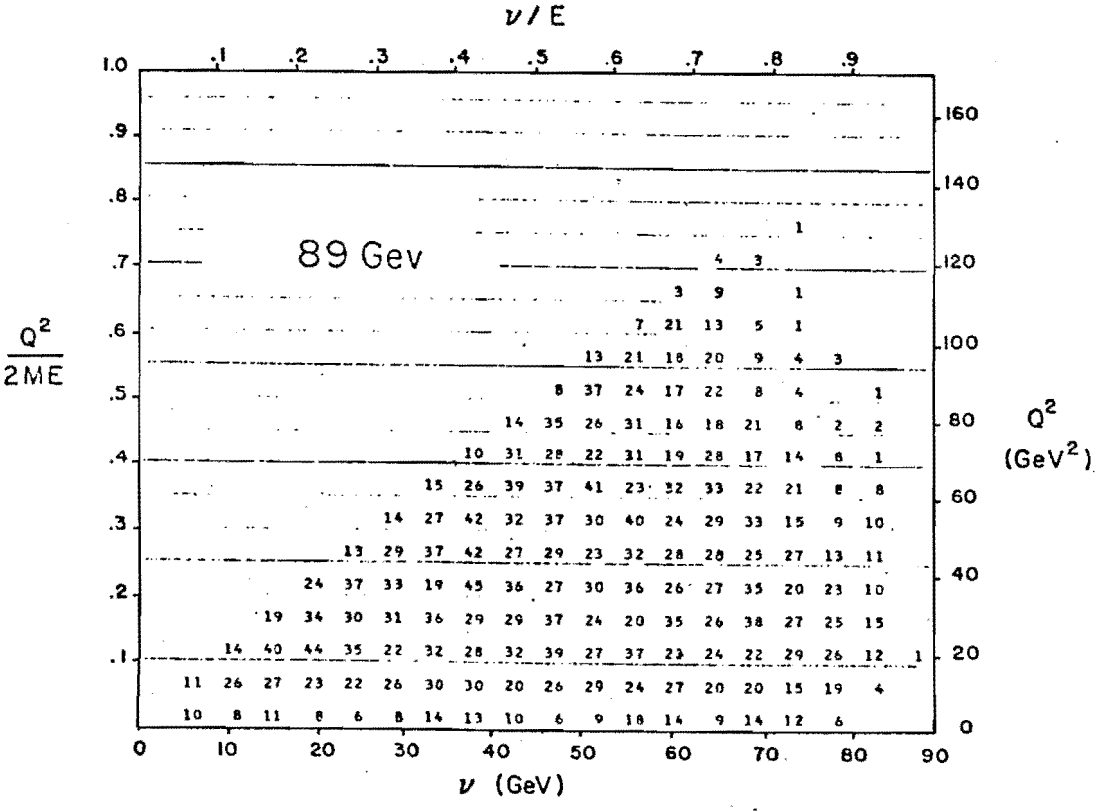


FIGURE A1b. Detection efficiency in the $Q^2$ - $\nu$ plane for $E_o$ = 89 GeV, with the apparatus in the 89-GeV scale-invariant configuration as described in P307. Unit acceptance is 100 events per bin.

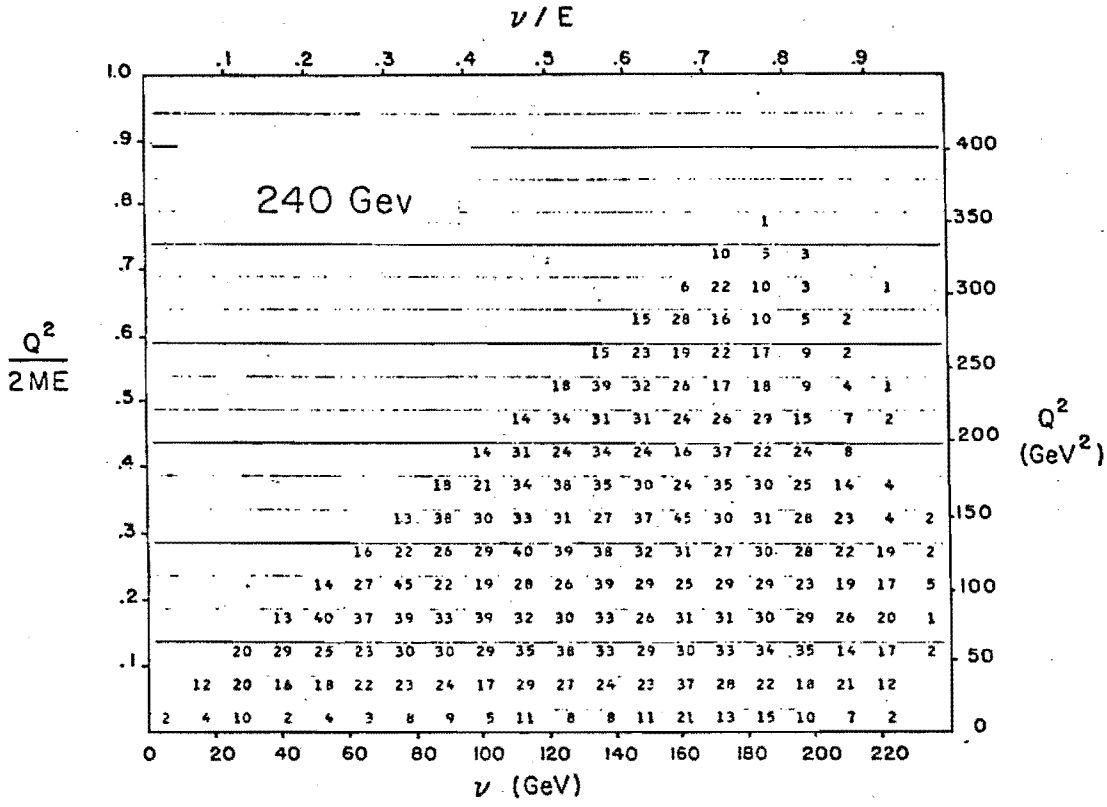


FIGURE A2. Detection efficiency in the $Q^2$ - $\nu$ plane for $E_o$ = 240 GeV, with the apparatus in the 200-GeV scale invariant configuration as described in P307. Unit acceptance is 100 events per bin.

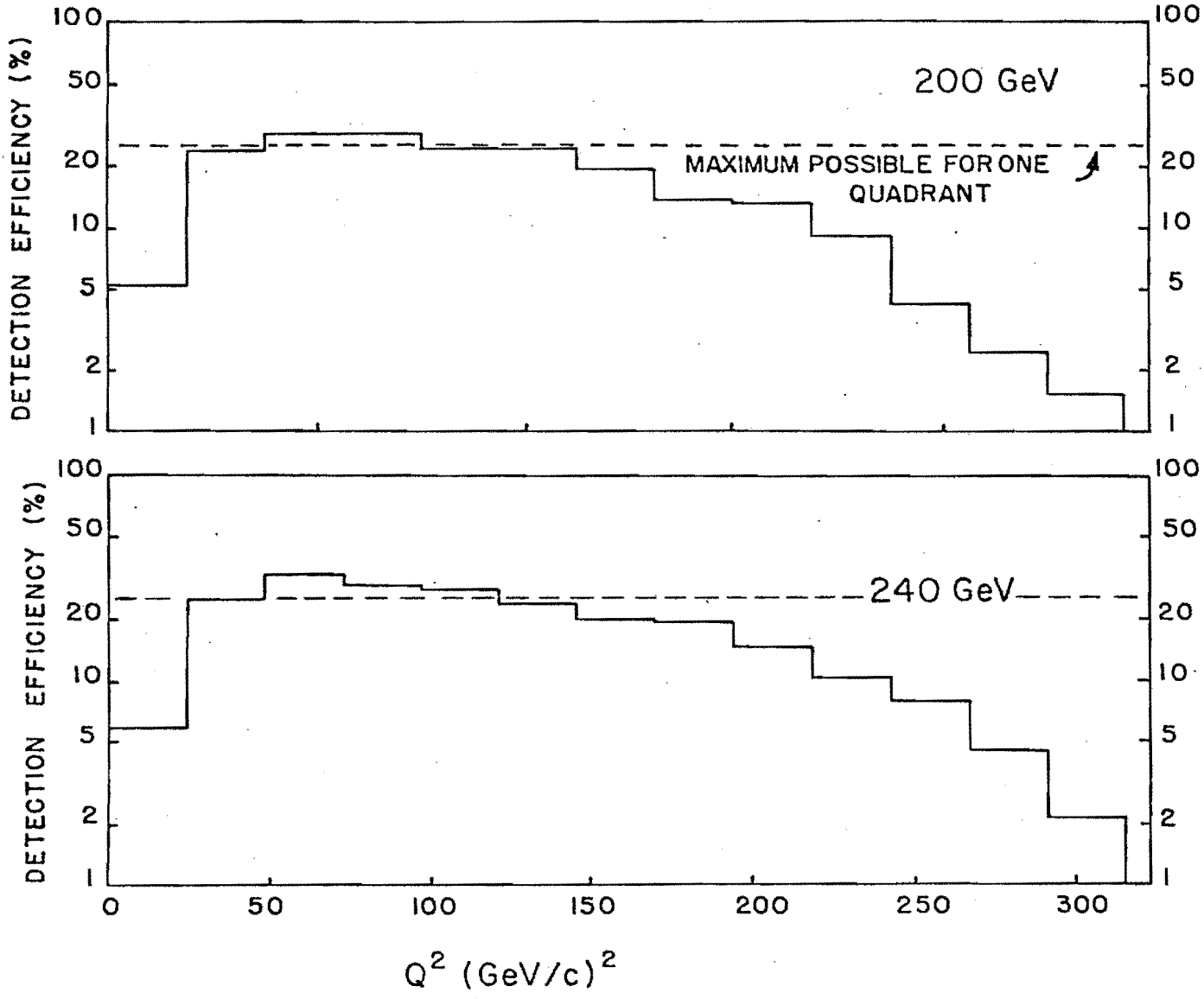


FIGURE A3. Detection efficiency vs. $Q^2$ for a) $E_o$ = 200 GeV and b) $E_o$ = 240 GeV. For both cases the apparatus was in the 200-GeV scale-invariant configuration as described in P307. See P307 main text and Appendix D for details of the calculation.

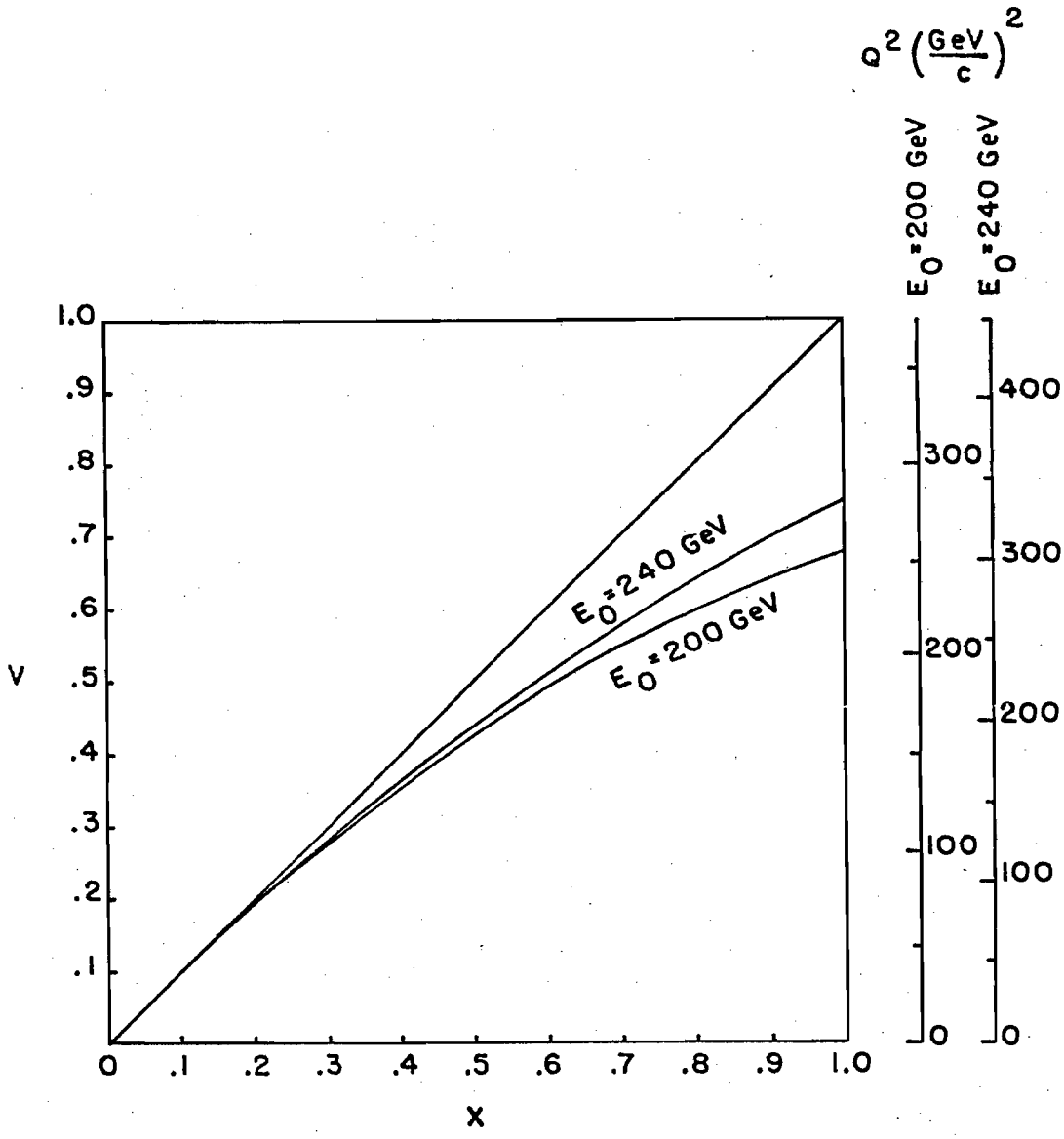


FIGURE A4. Acceptance region in the v-x plane for the apparatus of P307 at two incident energies. For both cases the apparatus was in the 200-GeV scale invariant configuration as described in the proposal. The kinematically allowed region is for $v \leq x$. For each incident energy the apparatus accepts events in the region below the indicated curve with an efficiency greater than 1/3 the maximum possible.

LAWRENCE RADIATION LABORATORY - UNIVERSITY OF CALIFORNIA

# ENGINEERING NOTE

Appendix AA

| AUTHOR | DEPARTMENT | LOCATION | DATE |
|---|---|---|---|
| J. Gunn | Mechanical Engineering | Berkeley | December 2, 1974 |

PROGRAM / PROJECT NO.

MECHANICAL ENGINEERING

COSTS, TIME STUDIES, ESTIMATING

TITLE

PARTIAL COST ESTIMATE FOR NAL EXP. #P307

B1

"A" Rev. 12/3/74 - D.F.R.

This cost estimate covers only the iron-target iron-magnet assembly, together with its zinc absorbers as described in the proposal of May 30, 1974 by A.R. Clark, et al. for NAL experiment P307.

MAGNET STEEL PLATES - AISI 1020

Informal quote - Lukens Steel Co., Coatsville, Pennsylvania
17.8¢/lb, 5 month delivery (subject to escalation)
Estimated freight to Chicago: 2¢/lb

| | |
|---|---|
| 72 plates at 9160 lb/plate × 19.8¢/lb . . . . . | $130,600 |
| Labor to flame cut 144 holes for coils - 6"×42" - 294 hours @ $15/hr . . . . . | 4,400 |
| Estimated freight Chicago to NAL @ 1¢/lb . . . . . | 6,600 |
| Lifting rig for plates . . . . . | 250 |
| Steel plate cost: | $141,850 |

ALUMINUM CONDUCTORS

Extruded alloy 1060F - 61% AICS conductivity
1.5"×0.75" with ½ diam. hole 1.1 lb/ft
50 turns @ 125 ft/turn = 6,250
Add 10% for spoilage 625
6,875 lb

Quote from New Jersey Alum Co., Elizabeth, N.J.

| | | |
|---|---|---|
| Tooling charge: | $450 | |
| Setup charge: | 140 | |
| Reels: | 936 | |
| | | $1,525 |
| Plus $1.035/lb × 6,875 lb . . . . . | | 7,115 |
| Plus estimated shipping to NAL @ 3¢/lb . . . . . | | 235 |
| Conductor cost: | | $8,865 |

## COIL FABRICATION

Aluminum hose barbs
8/turn × 50 turns = 400 required @ $1.05 ea. . . . . 425
Labor to weld to conductors
C'bore: 34 hrs
Weld: 40 hrs
74 hrs @ $15/hr . . . . . 1,125

Tape wrap conductors
half lap 2 layers Mylar tape
300 hours @ $15/hr . . . . . 4,500

Thermal switches
4 required at $35 each (installed) . . . . . 140

Flow switches
one required at $200 each (installed) . . . . . 200

Hoses - 200 required - 1 foot long
@ 50¢/ft . . . . . 100
Plus 400 hose clamps @ 75¢ ea. . . . . 300
Plus installation: 40 hours @ $15/hr . . . . . 600
Large supply hoses: 80 ft @ $2/ft . . . . . 160

Manifolds - two required
Materials . . . . . 100
Labor: 30 hours @ $15/hr . . . . . 450

Coil fabrication cost: $8,100

## MAGNET ASSEMBLY COSTS

| | | |
|---|---|---|
| Stack steel plates: | 150 man-hours | |
| Weld together: | 80 " | |
| Install coil: | 80 " | |
| Pressure & flow check: | 20 " | |
| Install steel for zinc tracks: | 40 " | |
| | 370 man-hours @ $15/hr . . . | $5,550 |

Material - 150 ft 4" channel (8 lb/ft) @ .50¢/lb
cut, drilled, and ready for install . . . . . 600
$6,150

## ZINC ABSORBER COSTS

Quote from Pacific Brass Foundry Co., San Francisco
36 required 4" × 42" × 51" - 2226 lb each
36 plates @ $1,745 each including material . . . . . $62,820

ENGINEERING DESIGN & DRAFTING

| | |
|---|---|
| 160 hours @ $20/hr . . . . . | $3,200 |

HANGERS & TRACKS FOR ZINC

| | |
|---|---|
| 144 bearings @ $4 . . . . . | 575 |
| 36 tracks @ 12 ft of steel/track is 432 ft of 3" I beam (7.5 lb/ft) is 3240 lb @ 50¢/lb cut, drilled, and ready for install . . . . . | 1,620 |

SUPPORT (BASE) FOR MAGNET

| | |
|---|---|
| Pour two concrete piers, 56 ft long each with stl. bar imbeded on top surface . . . . . | 2,500 |
| GRAND TOTAL: | $235,680 |
| Contingency 20% . . . . . | 47,136 |
| | $282,816 |

Inflation (should be provided for at about 1% per month for the appropriate time).

JG/ml

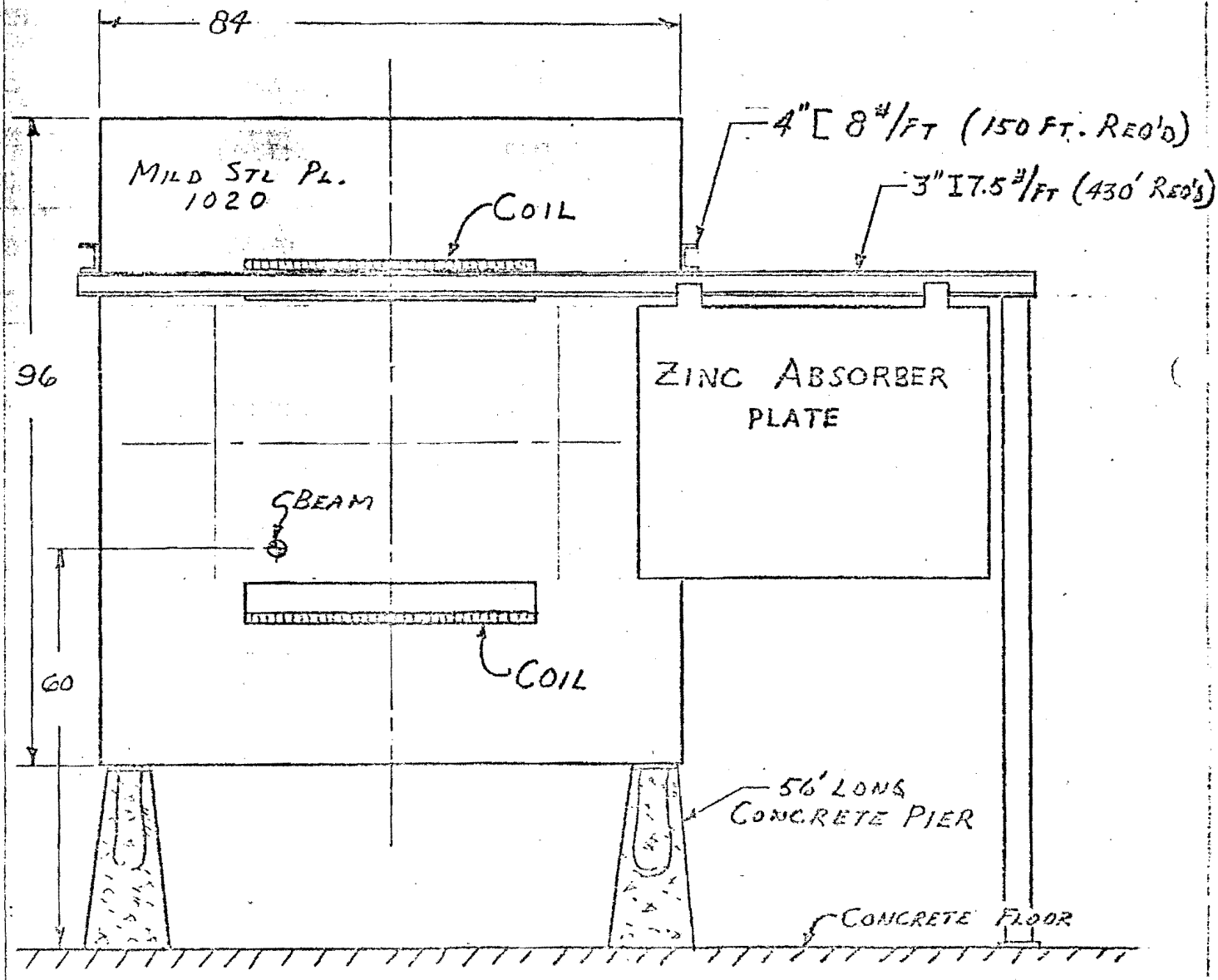


IRON TARGET - IRON MAGNET SKETCH

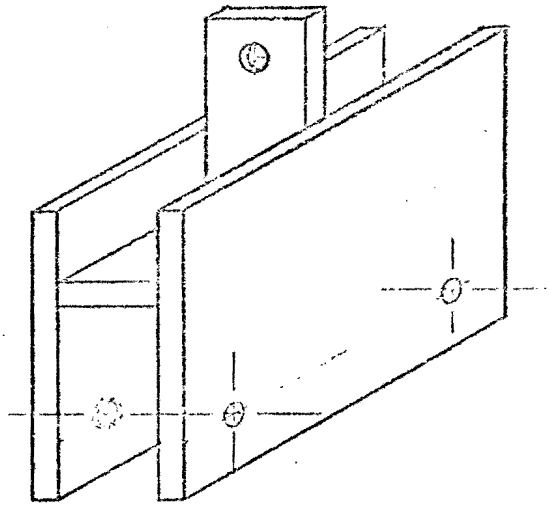

LIFTING RIG FOR STL. PLATES

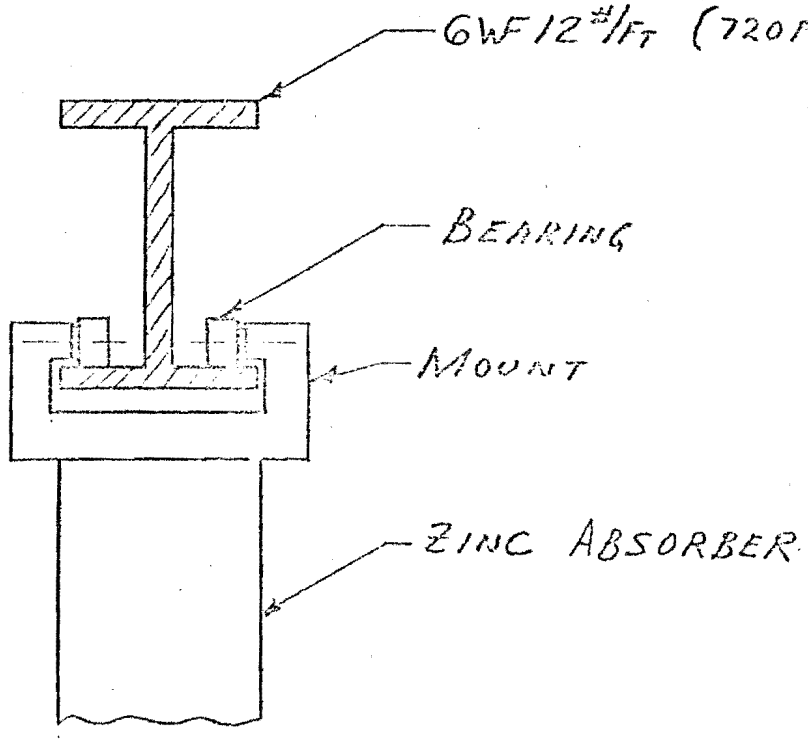


HANGER + TRACK FOR ZINC ABSORBER

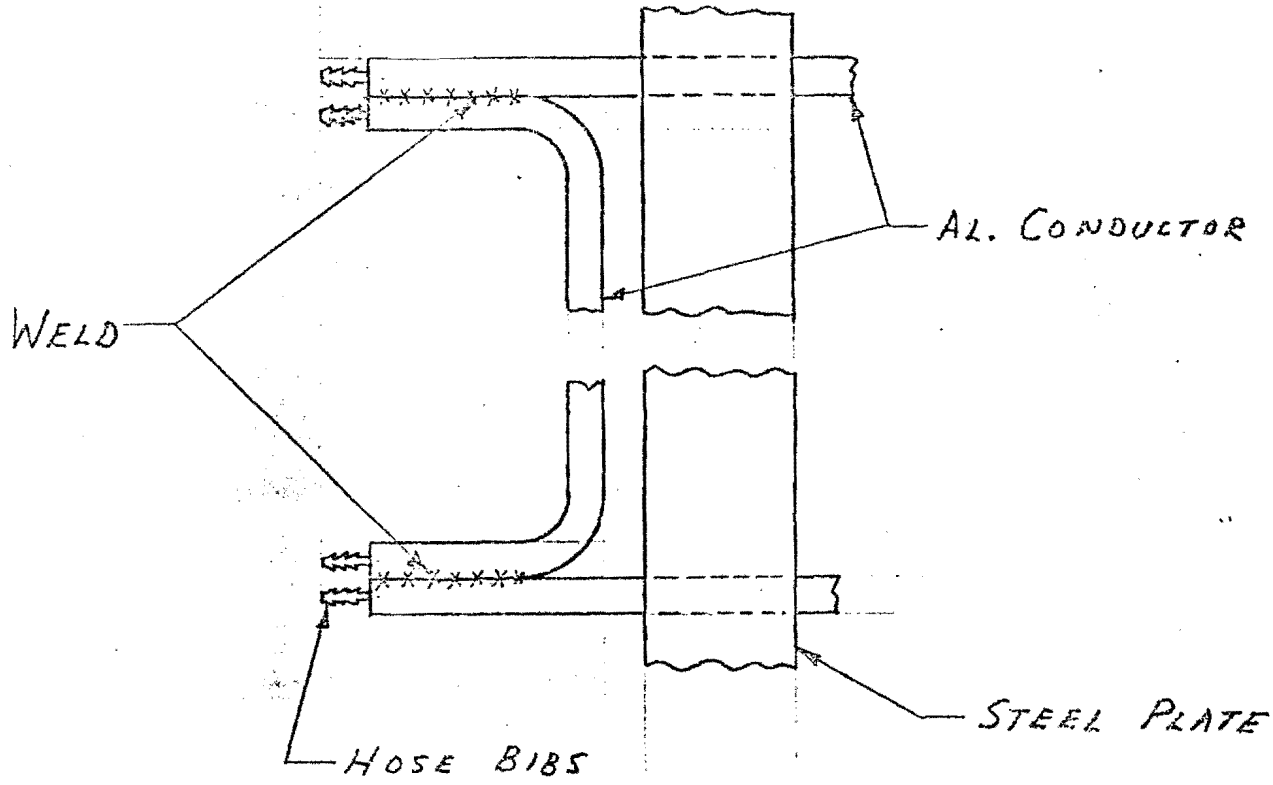


ELECTRICAL CROSS CONNECT SKETCH